Revision of the AF4 calibration experiment (Supplementary information)

Benedikt Häusele, Maxim B. Gindele, Helmut Cölfen

Contents

1 Determination of geometrical channel volume V^{geo}

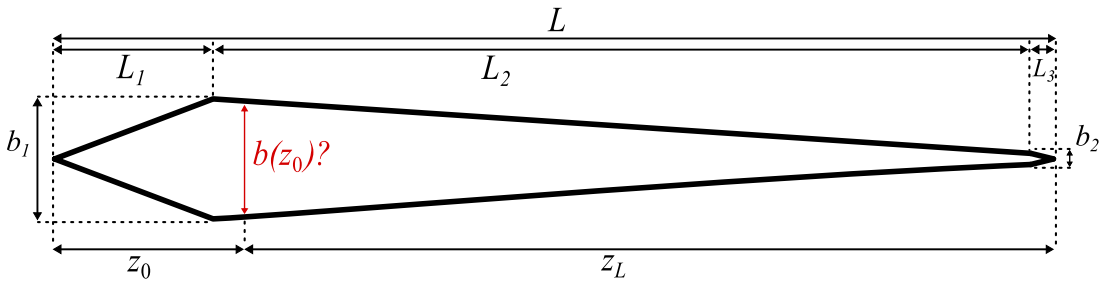

Fig. S.1.1: Channel dimensions. The width $b(z_L)$ depends on the focus position and is not accessible via geometrical channel data only.

AF4 channels have a trapezoidal shape with measures indicated in fig. S.1.1. For all further considerations, the channel plane is split into three sections (1,2,3) with their correspoding lengths L_1, L_2, L_3. To simplify the further calculations, they are subsumed as in the following:

$$L = L_1 + L_2 + L_3 = L_{12} + L_3 \tag{S.1.1}$$

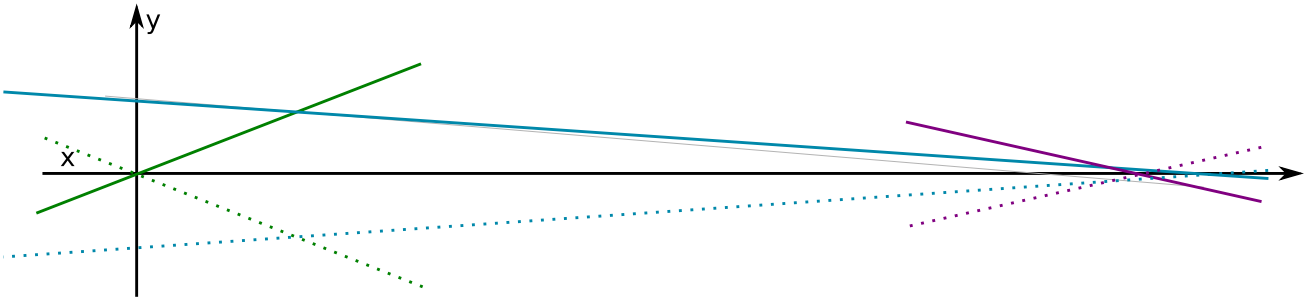

Fig. S.1.2: Channel dimensions as a set of 3 pairs of straight lines.

As the sample is focussed at a certain channel position on the beginning, this has to be considered. The relative focus position $z_{\%}$is related to the other focus-related magnitudes by

$$z_0 = z_{\%} L = L - z_L \tag{S.1.2}$$

The channel height difference $b_\Delta$on the section 2 is

$$b_\Delta = b_1 - b_2 \geqq 0 \tag{S.1.3}$$

Volume calculation may be conducted for the trapezoidal by simple decomposition of the channel plane into elementary geometrical objects. However, a concise analytical approach is more appropriate as the result can be displayed as a function of $z_{\%}$. In addition the corresponding $b(z_{\%})$ is not known initially. Similar derivations have already been conducted with the approximation of dividing the shape into two sections.[1–4] The approach may be useful for further hydrodynamic considerations as for example, the elution flow $V_e(x)$ in AF4 is a position-dependent size. For the trapezoidal plane shape, the channel is described by the enclosure of three pairs of straight line S.1.2. All expressions here are not optimized for mathematical elegance, but rather for being translated into an understandable and well-maintainable calculation routine. This is achieved by extensive subsitution of the known variables. Subsuming of these magnitudes helps to simplify the later expressions. In addition it allows the transformation and variation if a modification is required, for example if another shape model shall be introduced. Due to the reason of symmetry, only three borders have to be described exactly:

$$\frac{1}{2} b(x) = E(x) \begin{cases} e_1(x) = m_1 x = \frac{b_1}{2L_1} \cdot x & \forall \quad 0 \leqq x \leqq L_1 \\ e_2(x) = m_2 x + t_2 = -\frac{b_\Delta}{2L_2} \cdot x + \frac{1}{2}\left(b_1 + \frac{L_1}{L_2} b_\Delta\right) & \forall \quad L_1 < x \leqq L_{12} \\ e_3(x) = m_3 x + t_3 = -\frac{b_L}{2L_3} \cdot x + \frac{L b_L}{2L_3} & \forall \quad L_{12} < x \leqq L \end{cases} \tag{S.1.4}$$

As all dimensions here are known, the slopes and offsets of the lines can be calculated directly and don't have to be resubsituted after the following substitutions. The calcuation of geometrical volume of the trapezoidal channel has to be adapted according to whether the focus position z_0 is located left or right to the position of maximal channel extent (i.e. if $z_0 < L_1$ or $z_0 \geqq L_1$). In the algorithm later, rather the plane is used explicitly, which is obtained easily

V^{geo}: Distal focussing with $z_0 \geqq L_1$

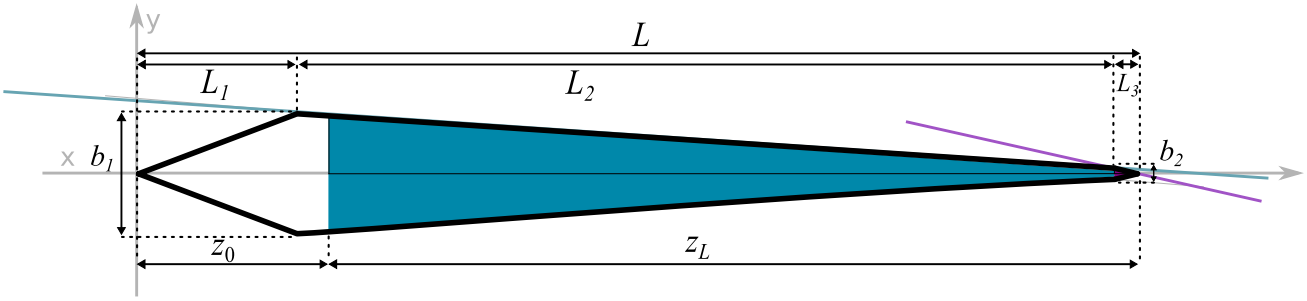

Fig. S.1.3: Area section passed by the sample during the measurement marked with the color of the corresponding line in the case of distal focussing

In this case, the channel volume V^{geo} is the product of the channel width w and the colored area the x, y-plane of Fig. S.1.3. It is described by:

$$\begin{aligned} V^{\text{geo}} &= \left(A_2 + A_3 \right) \cdot w \\ &= 2 \cdot \left(\int_{z_0}^{L_{12}} e_2(x)\,\mathrm{d}x + \int_{L-L_3}^{L} e_3(x)\,\mathrm{d}x \right) \cdot w \\ &= \left((L_{12} - z_0)\left(m_2\left(L_{12} + z_0\right) + 2t_2\right) + \tfrac{1}{2} \cdot L_3 \cdot b_L \right) \cdot w \end{aligned} \tag{S.1.5}$$

V^{geo}: Proximal focussing with $z_0 < L_1$

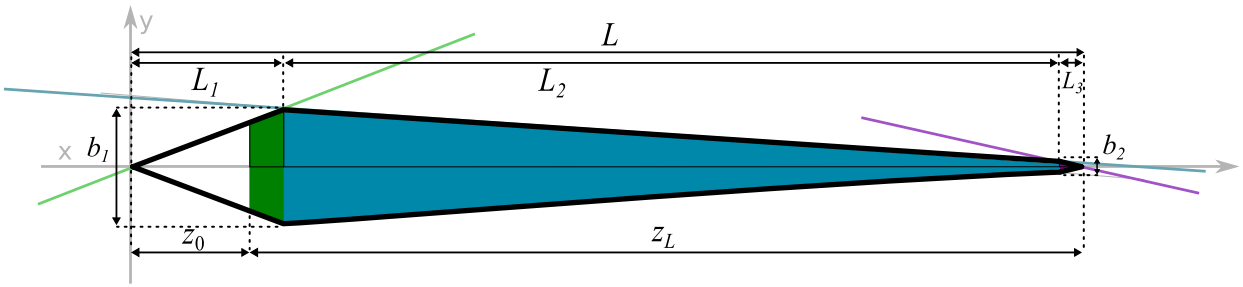

Fig. S.1.4: Area section passed by the sample during the measurement marked with the color of the corresponding line in the case of proximal focussing

Outgoing from the previous result, the full area section of section 2 has to be considered, i.e. first z_0 is replaced by L_1, then the area part of section 1 is added:

$$\begin{aligned} V^{\text{geo}} &= \left(A_1 + A_2 + A_3 \right) \cdot w \\ &= 2 \cdot \left(\int_{z_0}^{L_1} e_1(x)\,\mathrm{d}x + \int_{L_1}^{L_{12}} e_2(x)\,\mathrm{d}x + \int_{L-L_3}^{L} e_3(x)\,\mathrm{d}x \right) \cdot w \\ &= \left(m_1 \cdot (L_1^2 - z_0^2) + m_2 L_{12} L_2 + m_2 L_1 L_2 + 2t_2 L_2 + \tfrac{1}{2} \cdot L_3 \cdot b_L \right) \cdot w \\ &= \left(m_1 \cdot (L_1^2 - z_0^2) + \tfrac{1}{2}(b_1 + b_2) L_2 + \tfrac{1}{2} \cdot L_3 \cdot b_L \right) \cdot w \end{aligned} \tag{S.1.6}$$

2 Determination of "hydrodynamic" channel height w^{hyd} and volume V^{hyd}

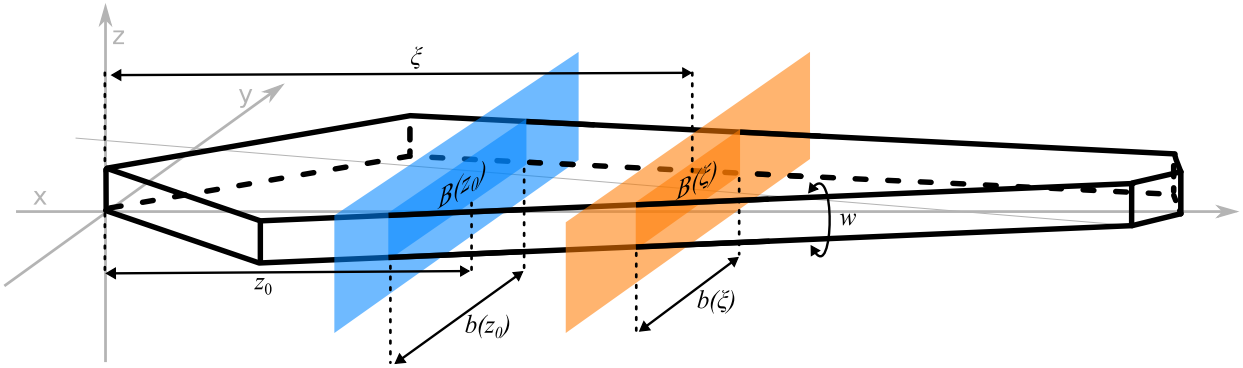

Fig. S.2.1: Cross sections $B(\xi)$ of the channel at different positions ξ

Here, the derivation is analogously conducted as described in literature[1, 5, 6], but using the straight equations S.1.4 for description of the channel above. The simplified version according to Litzén and Wahlund[6] is given in the section below. Although our approach is physically equivalent to the ideas of cited reference, our formulation has 3 advantages: First, we do not have to extrapolate for external points. Secondly, our formulation is more flexible and can be adapted easily to other possible channel shapes by simply adapting $E(x)$. Here the strict analytical formulation of the channel shape instead of using elementary geometry is advantageous. A last, our formulation gives direct access to w as a target size for calibration.

The approach takes into consideration that $b(z)$ is variable over the whole channel length. In addition, also focussing into the first channel section is considered. For this reason, the surface cannot just be corrected by a constant term as reported earlier. [6] t_{void} is the hypothetical time of a species to pass the separation volume with the mean migration velocity. It can be obtained by integration over the channel positions ξ. Although this derivation leads to rather laborious expressions, it has the advantage that no additional assumptions are necessary.

$$t_{\mathrm{void}} = \int_0^{t_{\mathrm{void}}} \mathrm{d}t = \int_{z_0}^{L} \frac{1}{v_{\mathrm{m}}(\xi)}\,\mathrm{d}\xi \tag{S.2.1}$$

$v_{\mathrm{m}}(\xi)$ is the migration velocity of the eluent at a channel position ξ. It dependends on the flow velocity $\dot{V}(\xi)$ at the position and the y, z cross-sectional area $B(\xi)$ at (Fig S.2.1)

$$v_{\mathrm{m}}(\xi) = \frac{\dot{V}(\xi)}{B(\xi)} = \frac{\dot{V}(\xi)}{b(\xi)\cdot w} \tag{S.2.2}$$

The term $b(\xi)$ is described with the aid of eq. S.1.4 and will require a case-by-case approach. The change of the flow velocity $\dot{V}(\xi)$ is exactly the total loss in the applied crossflow. It has its maximum at the inlet position with

$$\dot{V}(0) = \dot{V}_{\mathrm{in}} = \dot{V}_{\mathrm{e}} + \dot{V}_{\mathrm{c}} \tag{S.2.3}$$

and its minimum with

$$\dot{V}(L) = \dot{V}_{\mathrm{e}} \tag{S.2.4}$$

As this is distributed uniformly over the membrane surface, the decay is proportional to the area the eluent has already passed. This leads to the expression

$$\dot{V}(\xi) = \dot{V}_{\text{in}} - V_c \cdot \frac{A(\xi)}{A_L} = \dot{V}_{\text{in}} - V_c \cdot \frac{\int_0^{\xi} b(x)\,\mathrm{d}x}{\int_0^{L} b(x)\,\mathrm{d}x} = \dot{V}_{\text{in}} - V_c \cdot \frac{2 \cdot \int_0^{\xi} E(x)\,\mathrm{d}x}{A_L} \tag{S.2.5}$$

The total area $A_L$can be easily derived by letting of eq. S.1.6 with letting $z_0 = 0$:

$$A_L = \boxed{A_1} + \boxed{A_2} + \boxed{A_3} = \boxed{\tfrac{1}{2} b_1 L_1} + \boxed{\tfrac{1}{2}(b_1 + b_2) L_2} + \boxed{\tfrac{1}{2} L_3 b_2} \tag{S.2.6}$$

To evaluate $A(\xi)$ correctly, the integrals have to be split according to the conditions in eq. S.1.4. This requirement corresponds to the cases same needed for $b(\xi)$, i.e. the different passed channel sections. Merging eq. S.2.1 and S.2.5 gives the expression

$$v_{\text{m}}(\xi) = \frac{\dot{V}_{\text{in}} - V_c \cdot \frac{2 \cdot \int_0^{\xi} E(x)\,\mathrm{d}x}{A_L}}{2 \cdot E(\xi) \cdot w} = \frac{1}{2 \cdot w} \cdot \frac{\dot{V}_{\text{in}} - V_c \cdot \frac{2 \cdot \int_0^{\xi} E(x)\,\mathrm{d}x}{A_L}}{E(\xi)} \tag{S.2.7}$$

Inserting into eq. S.2.1 gives:

$$t_{\text{void}} = 2 \cdot w \cdot \int_{z_0}^{L} \frac{E(\xi)}{\dot{V}_{\text{in}} - V_c \cdot \frac{2 \cdot \int_0^{\xi} E(x)\,\mathrm{d}x}{A_L}}\,\mathrm{d}\xi \tag{S.2.8}$$

This expression quantifies a linear conversion factor C_{F} for the relationship of t_{void} and w. This promises a simple relationship between those two basic magnitudes with

$$t_{\text{void}} = 2 \cdot C_{\text{F}} \cdot w \tag{S.2.9}$$

and

$$C_{\text{F}} = \int_{z_0}^{L} \frac{E(\xi)}{\dot{V}_{\text{in}} - V_c \cdot \frac{2 \cdot \int_0^{\xi} E(x)\,\mathrm{d}x}{A_L}}\,\mathrm{d}\xi \tag{S.2.10}$$

Similar to the calculation of V^{geo} above, a case-by case analysis is required depending on z_0. Due to the section-wise definition of the integrand, the integrals then have to be split accordingly to the partial domain of $E(\xi)$.

V^{hyd}: Distal focussing with $z_0 \geqq L_1$

Here, the outer integral of eq. S.2.8 is split into the sections with $L_1 < \xi \leqq L_{12}$ and $L_{12} < \xi$:

$$C_\mathrm{F} = \int_{z_0}^{L_{12}} \frac{E(\xi)}{\dot{V}_\mathrm{in} - \dfrac{2V_c}{A_L}\displaystyle\int_0^{\xi} E(x)\,\mathrm{d}x}\,\mathrm{d}\xi + \int_{L_{12}}^{L} \frac{E(\xi)}{\dot{V}_\mathrm{in} - \dfrac{2V_c}{A_L}\displaystyle\int_0^{\xi} E(x)\,\mathrm{d}x}\,\mathrm{d}\xi \tag{S.2.11}$$

As ξ is now located only on one of the section within each summand, the inner integrals can be split for the different domains of $E(x)$. Integrals independent from ξ are directly substituted with their corresponding area section from eq. S.2.6, only the last integral is solved.

$$\begin{aligned} C_\mathrm{F} \;=\; & \int_{z_0}^{L_{12}} \frac{e_2(\xi)}{\dot{V}_\mathrm{in} - \dfrac{2V_c}{A_L}\left(\displaystyle\int_0^{L_1} e_1(x)\,\mathrm{d}x + \int_{L_1}^{\xi} e_2(x)\,\mathrm{d}x\right)}\,\mathrm{d}\xi \\ & + \int_{L_{12}}^{L} \frac{e_3(\xi)}{\dot{V}_\mathrm{in} - \dfrac{2V_c}{A_L}\left(\displaystyle\int_0^{L_1} e_1(x)\,\mathrm{d}x + \int_{L_1}^{L_{12}} e_2(x)\,\mathrm{d}x + \int_{L_{12}}^{\xi} e_3(x)\,\mathrm{d}x\right)}\,\mathrm{d}\xi \\ = \; & \int_{z_0}^{L_{12}} \frac{m_2\cdot\xi + t_2}{\dot{V}_\mathrm{in} - \dfrac{2V_c}{A_L}\left(\dfrac{1}{2}A_1 + \dfrac{1}{2}m_2(\xi^2 - L_1^2) + t_2(\xi - L_1)\right)}\,\mathrm{d}\xi \\ & + \int_{L_{12}}^{L} \frac{m_3\cdot\xi + t_3}{\dot{V}_\mathrm{in} - \dfrac{2V_c}{A_L}\left(\dfrac{1}{2}A_1 + \dfrac{1}{2}A_2 + \dfrac{1}{2}m_3(\xi^2 - L_{12}^2) + t_3(\xi - L_{12})\right)}\,\mathrm{d}\xi \end{aligned} \tag{S.2.12}$$

In order to transform the integrand terms into ordinary rational functions and simplify the analytical solutions, this can be rearranged by using substitutions for the occurring prefactors $\alpha_i, \beta_i, \gamma_i, \delta_i$, the quadratic polynomials $P(\xi)$ and its discriminants Δ_i:

$$\begin{aligned} &\alpha_2 = \tfrac{t_2}{m_2} \quad \beta_2 = -\tfrac{\dot{V}_c m_2}{A_L} \quad \gamma_2 = -\tfrac{2\dot{V}_c t_2}{A_L} \\ &\delta_2 = \dot{V}_\mathrm{in} - \tfrac{\dot{V}_c}{A_L}\left(A_1 - m_2 L_1^2 - 2t_2 L_1\right) \qquad \Delta_2 = 4\beta_2\delta_2 - \gamma_2^2 \\ &\alpha_3 = \tfrac{t_3}{m_3} \quad \beta_3 = -\tfrac{\dot{V}_c m_3}{A_L} \quad \gamma_3 = -\tfrac{2\dot{V}_c t_3}{A_L} \\ &\delta_3 = \dot{V}_\mathrm{in} - \tfrac{\dot{V}_c}{A_L}\left(A_1 + A_2 - m_3 L_{12}^2 - 2t_3 L_{12}\right) \quad \Delta_3 = 4\beta_3\delta_3 - \gamma_3^2 \end{aligned} \tag{S.2.13}$$

$$\begin{aligned} P_2(\xi) &= \beta_2\xi^2 + \gamma_2\xi + \delta_2 \\ P_3(\xi) &= \beta_3\xi^2 + \gamma_3\xi + \delta_3 \end{aligned} \tag{S.2.14}$$

For solving the integral it is important to know the sign of Δ_2 and Δ_3. Inserting S.2.3, it can be shown (see below) that it is not possible to determine the scope of Δ_2 exactly for the general case and the case-by-case analysis has to be conducted "at runtime". To simplify the display of this expression, it is split and each summand treated separately:

$$C_\mathrm{F} = C_\mathrm{F2} + C_\mathrm{F3} \tag{S.2.15}$$

$$
\begin{aligned}
C_{\mathrm{F}2} &= m_2 \cdot \int_{z_0}^{L_{12}} \frac{\xi+\alpha_2}{\beta_2\xi^2+\gamma_2\xi+\delta_2}\,\mathrm{d}\xi \\
&= m_2 \cdot \left(\int_{z_0}^{L_{12}} \frac{\xi}{P_2(\xi)}\,\mathrm{d}\xi + \int_{z_0}^{L_{12}} \frac{\alpha_2}{P_2(\xi)}\,\mathrm{d}\xi \right) \\
&= m_2 \cdot \left(\left[\tfrac{\ln P_2(\xi)}{2\beta_2}\right]_{z_0}^{L_{12}} + \left(\alpha_2 - \tfrac{\gamma_2}{2\beta_2}\right) \int_{z_0}^{L_{12}} \frac{\mathrm{d}\xi}{P_2(\xi)} \right) \qquad [7] \\
&= \begin{cases} m_2 \cdot \left(\left[\tfrac{\ln P_2(\xi)}{2\beta_2}\right]_{z_0}^{L_{12}} + \left(\alpha_2 - \tfrac{\gamma_2}{2\beta_2}\right) \left[\tfrac{2}{\sqrt{\Delta_2}} \cdot \operatorname{arctan}\left(\tfrac{2\beta_2\xi+\gamma_2}{\sqrt{\Delta_2}} \right) \right]_{z_0}^{L_{12}} \right) & \forall \Delta_2 > 0 \\ m_2 \cdot \left(\left[\tfrac{\ln P_2(\xi)}{2\beta_2}\right]_{z_0}^{L_{12}} + \left(\alpha_2 - \tfrac{\gamma_2}{2\beta_2}\right) \left[-\tfrac{2}{\sqrt{-\Delta_2}} \cdot \operatorname{artanh}\left(\tfrac{2\beta_2\xi+\gamma_2}{\sqrt{-\Delta_2}} \right) \right]_{z_0}^{L_{12}} \right) & \forall \Delta_2 < 0 \end{cases} \qquad [8] \\
&= \begin{cases} m_2 \cdot \left(\tfrac{1}{2\beta_2}\left(\ln P_2(L_{12}) - \ln P_2(z_0)\right) + \left(\tfrac{2}{\sqrt{\Delta_2}}\right)\left(\alpha_2 - \tfrac{\gamma_2}{2\beta_2}\right)\left(\arctan \tfrac{2\beta_2 L_{12}+\gamma_2}{\sqrt{\Delta_2}} - \arctan \tfrac{2\beta_2 z_0+\gamma_2}{\sqrt{\Delta_2}} \right) \right) & \forall \Delta_2 > 0 \\ m_2 \cdot \left(\tfrac{1}{2\beta_2}\left(\ln P_2(L_{12}) - \ln P_2(z_0)\right) - \left(\tfrac{2}{\sqrt{-\Delta_2}}\right)\left(\alpha_2 - \tfrac{\gamma_2}{2\beta_2}\right)\left(\operatorname{artanh} \tfrac{2\beta_2 L_{12}+\gamma_2}{\sqrt{-\Delta_2}} - \operatorname{artanh} \tfrac{2\beta_2 z_0+\gamma_2}{\sqrt{-\Delta_2}} \right) \right) & \forall \Delta_2 < 0 \end{cases} \\
&= \begin{cases} m_2 \cdot \left(\tfrac{1}{2\beta_2} \ln \tfrac{P_2(L_{12})}{P_2(z_0)} + \left(\tfrac{2}{\sqrt{\Delta_2}}\right)\left(\alpha_2 - \tfrac{\gamma_2}{2\beta_2}\right)\left(\arctan \tfrac{2\beta_2 L_{12}+\gamma_2}{\sqrt{\Delta_2}} - \arctan \tfrac{2\beta_2 z_0+\gamma_2}{\sqrt{\Delta_2}} \right) \right) & \forall \Delta_2 > 0 \\ m_2 \cdot \left(\tfrac{1}{2\beta_2} \ln \tfrac{P_2(L_{12})}{P_2(z_0)} - \left(\tfrac{2}{\sqrt{-\Delta_2}}\right)\left(\alpha_2 - \tfrac{\gamma_2}{2\beta_2}\right)\left(\operatorname{artanh} \tfrac{2\beta_2 L_{12}+\gamma_2-2\beta_2 z_0-\gamma_2}{\sqrt{-\Delta_2}\cdot\left(1-\frac{2\beta_2 L_{12}+\gamma_2}{\sqrt{-\Delta_2}}\cdot\frac{2\beta_2 z_0+\gamma_2}{\sqrt{-\Delta_2}}\right)} \right) \right) & \forall \Delta_2 < 0 \end{cases} \\
&= \begin{cases} m_2 \cdot \left(\tfrac{1}{2\beta_2} \ln \tfrac{P_2(L_{12})}{P_2(z_0)} + \left(\tfrac{2}{\sqrt{\Delta_2}}\right)\left(\alpha_2 - \tfrac{\gamma_2}{2\beta_2}\right)\left(\arctan \tfrac{2\beta_2 L_{12}+\gamma_2}{\sqrt{\Delta_2}} - \arctan \tfrac{2\beta_2 z_0+\gamma_2}{\sqrt{\Delta_2}} \right) \right) & \forall \Delta_2 > 0 \\ m_2 \cdot \left(\tfrac{1}{2\beta_2} \ln \tfrac{P_2(L_{12})}{P_2(z_0)} - \left(\tfrac{2}{\sqrt{-\Delta_2}}\right)\left(\alpha_2 - \tfrac{\gamma_2}{2\beta_2}\right)\left(\operatorname{artanh} \tfrac{2\beta_2(L_{12}-z_0)}{\left(\sqrt{-\Delta_2} - \frac{(2\beta_2 L_{12}+\gamma_2)(2\beta_2 z_0+\gamma_2)}{\sqrt{-\Delta_2}}\right)} \right) \right) & \forall \Delta_2 < 0 \end{cases}
\end{aligned}
\qquad \text{(S.2.16)}
$$

$$
\begin{aligned}
C_{\mathrm{F}3} &= m_3 \cdot \int_{L_{12}}^{L} \frac{\xi+\alpha_3}{\beta_3\xi^2+\gamma_3\xi+\delta_3}\,\mathrm{d}\xi \\
&= m_3 \cdot \left(\int_{L_{12}}^{L} \frac{\xi}{P_3(\xi)}\,\mathrm{d}\xi + \int_{L_{12}}^{L} \frac{\alpha_3}{P_3(\xi)}\,\mathrm{d}\xi \right) \\
&\quad \cdots \text{ analogously to eq. S.2.16 } \cdots \\
&= \begin{cases} m_3 \cdot \left(\tfrac{1}{2\beta_3} \ln \tfrac{P_3(L)}{P_3(L_{12})} + \left(\tfrac{2}{\sqrt{\Delta_3}}\right)\left(\alpha_3 - \tfrac{\gamma_3}{2\beta_3}\right)\left(\arctan \tfrac{2\beta_3 L+\gamma_3}{\sqrt{\Delta_3}} - \arctan \tfrac{2\beta_3 L_{12}+\gamma_3}{\sqrt{\Delta_3}} \right) \right) & \forall \Delta_3 > 0 \\ m_3 \cdot \left(\tfrac{1}{2\beta_3} \ln \tfrac{P_3(L)}{P_3(L_{12})} - \left(\tfrac{2}{\sqrt{-\Delta_3}}\right)\left(\alpha_3 - \tfrac{\gamma_3}{2\beta_3}\right)\left(\operatorname{artanh} \tfrac{2\beta_3(L-L_{12})}{\left(\sqrt{-\Delta_3} - \frac{(2\beta_3 L+\gamma_3)(2\beta_3 L_{12}+\gamma_3)}{\sqrt{-\Delta_3}}\right)} \right) \right) & \forall \Delta_3 < 0 \end{cases} \\
&= \begin{cases} m_3 \cdot \left(\tfrac{1}{2\beta_3} \ln \tfrac{P_3(L)}{P_3(L_{12})} + \left(\tfrac{2}{\sqrt{\Delta_3}}\right)\left(\alpha_3 - \tfrac{\gamma_3}{2\beta_3}\right)\left(\arctan \tfrac{2\beta_3 L+\gamma_3}{\sqrt{\Delta_3}} - \arctan \tfrac{2\beta_3 L_{12}+\gamma_3}{\sqrt{\Delta_3}} \right) \right) & \forall \Delta_3 > 0 \\ m_3 \cdot \left(\tfrac{1}{2\beta_3} \ln \tfrac{P_3(L)}{P_3(L_{12})} - \left(\tfrac{2}{\sqrt{-\Delta_3}}\right)\left(\alpha_3 - \tfrac{\gamma_3}{2\beta_3}\right)\left(\operatorname{artanh} \tfrac{2\beta_3\,(L-L_{12})}{\left(\sqrt{-\Delta_3} - \frac{(2\beta_3 L+\gamma_3)(2\beta_3 L_{12}+\gamma_3)}{\sqrt{-\Delta_3}}\right)} \right) \right) & \forall \Delta_3 < 0 \end{cases}
\end{aligned}
\qquad \text{(S.2.17)}
$$

V^{hyd}: Proximal focusing with $z_0 < L_1$

If the sample was focused to a point with $z_0 < L_1$, the in addition to the solution above, also the eluent migration through the first sections has to be considered. The evaluation of the expression can be conducted analogously for the second and third summand as shown above with adaption of the lower limit of integration for the second:

$$\begin{aligned}
C_{\mathrm{F}} &= \int_{z_0}^{L_1} \frac{e_1(\xi)}{\dot{V}_{\mathrm{in}} - \frac{2V_c}{A_L}\left(\int_0^{\xi} e_1(x)\,\mathrm{d}x\right)}\,\mathrm{d}\xi \\
&+ \int_{L_1}^{L_{12}} \frac{e_2(\xi)}{\dot{V}_{\mathrm{in}} - \frac{2V_c}{A_L}\left(\int_0^{L_1} e_1(x)\,\mathrm{d}x + \int_{L_1}^{\xi} e_2(x)\,\mathrm{d}x\right)}\,\mathrm{d}\xi \\
&+ \int_{L_{12}}^{L} \frac{e_3(\xi)}{\dot{V}_{\mathrm{in}} - \frac{2V_c}{A_L}\left(\int_0^{L_1} e_1(x)\,\mathrm{d}x + \int_{L_1}^{L_{12}} e_2(x)\,\mathrm{d}x + \int_{L_{12}}^{\xi} e_3(x)\,\mathrm{d}x\right)}\,\mathrm{d}\xi \\
&= \int_{z_0}^{L_1} \frac{m_1 \cdot \xi}{\dot{V}_{\mathrm{in}} - \frac{2V_c}{A_L}\left(\frac{1}{2}m_1\xi^2\right)}\,\mathrm{d}\xi \\
&+ \int_{L_1}^{L_{12}} \frac{m_2 \cdot \xi + t_2}{\dot{V}_{\mathrm{in}} - \frac{2V_c}{A_L}\left(\frac{1}{2}A_1 + \frac{1}{2}m_2(\xi^2 - L_1^2) + t_2(\xi - L_1)\right)}\,\mathrm{d}\xi \\
&+ \int_{L_{12}}^{L} \frac{m_3 \cdot \xi + t_3}{\dot{V}_{\mathrm{in}} - \frac{2V_c}{A_L}\left(\frac{1}{2}A_1 + \frac{1}{2}A_2 + \frac{1}{2}m_3(\xi^2 - L_{12}^2) + t_3(\xi - L_{12})\right)}\,\mathrm{d}\xi
\end{aligned} \tag{S.2.18}$$

Substitution is done similarly as above:

$$\begin{aligned}
&\beta_1 = -\tfrac{\dot{V}_c m_1}{A_L} \quad \delta_1 = \dot{V}_{\mathrm{in}} \\
\alpha_2 = \tfrac{t_2}{m_2} \quad &\beta_2 = -\tfrac{\dot{V}_c m_2}{A_L} \quad \gamma_2 = -\tfrac{2\dot{V}_c t_2}{A_L} \\
\delta_2 = \dot{V}_{\mathrm{in}} - \tfrac{\dot{V}_c}{A_L}&\left(A_1 - m_2 L_1^2 - 2t_2 L_1\right) \qquad \Delta_2 = 4\beta_2\delta_2 - \gamma_2^2 \\
\alpha_3 = \tfrac{t_3}{m_3} \quad &\beta_3 = -\tfrac{\dot{V}_c m_3}{A_L} \quad \gamma_3 = -\tfrac{2\dot{V}_c t_3}{A_L} \\
\delta_3 = \dot{V}_{\mathrm{in}} - \tfrac{\dot{V}_c}{A_L}&\left(A_1 + A_2 - m_3 L_{12}^2 - 2t_3 L_{12}\right) \quad \Delta_3 = 4\beta_3\delta_3 - \gamma_3^2
\end{aligned} \tag{S.2.19}$$

$$\begin{aligned}
P_2(\xi) &= \beta_2\xi^2 + \gamma_2\xi + \delta_2 \\
P_3(\xi) &= \beta_3\xi^2 + \gamma_3\xi + \delta_3
\end{aligned} \tag{S.2.20}$$

Then, in analogy, to the case $z_0 \geqq L_1$, C_F can be expressed as

$$\begin{aligned} C_\mathrm{F} &= C_{\mathrm{F}1} + C_{\mathrm{F}2} + C_{\mathrm{F}3} \\ &= m_1 \cdot \int_{z_0}^{L_1} \left(\frac{\xi}{\beta_1 \cdot \xi^2 + \delta_1} \right) \mathrm{d}\xi \\ &+ m_2 \cdot \int_{L_1}^{L_{12}} \left(\frac{\xi + \alpha_2}{\beta_2 \xi^2 + \gamma_2 \xi + \delta_2} \right) \mathrm{d}\xi \\ &+ m_3 \cdot \int_{L_{12}}^{L} \left(\frac{\xi + \alpha_3}{\beta_3 \xi^2 + \gamma_3 \xi + \delta_3} \right) \mathrm{d}\xi \end{aligned} \tag{S.2.21}$$

with

$$\begin{aligned} C_{\mathrm{F}1} &= m_1 \cdot \int_{z_0}^{L_1} \left(\frac{\xi}{\beta_1 \cdot \xi^2 + \delta_1} \right) \mathrm{d}\xi \\ &= \tfrac{m_1}{\beta_1} \cdot \int_{z_0}^{L_1} \left(\frac{\xi}{\frac{\delta_1}{\beta_1} + \xi^2 W} \right) \mathrm{d}\xi \\ &= \frac{m_1}{\beta_1} \cdot \tfrac{1}{2} \left[\ln\left(\left| \frac{\delta_1}{\beta_1} + \xi^2 \right| \right) \right]_{z_0}^{L_1} \\ &= \frac{m_1}{2\beta_1} \cdot \left(\ln \left| \frac{\delta_1}{\beta_1} + L_1^2 \right| - \ln \left| \frac{\delta_1}{\beta_1} + z_0^2 \right| \right) \end{aligned} \tag{S.2.22}$$

$$C_{\mathrm{F}2} = \begin{cases} m_2 \cdot \left(\frac{1}{2\beta_2} \ln \frac{P_2(L_{12})}{P_2(L_1)} + \left(\frac{2}{\sqrt{\Delta_2}} \right) \left(\alpha_2 - \frac{\gamma_2}{2\beta_2} \right) \left(\arctan \frac{2\beta_2 L_{12} + \gamma_2}{\sqrt{\Delta_2}} - \arctan \frac{2\beta_2 L_1 + \gamma_2}{\sqrt{\Delta_2}} \right) \right) & \forall \Delta_2 > 0 \\ m_2 \cdot \left(\frac{1}{2\beta_2} \ln \frac{P_2(L_{12})}{P_2(L_1)} - \left(\frac{2}{\sqrt{-\Delta_2}} \right) \left(\alpha_2 - \frac{\gamma_2}{2\beta_2} \right) \left(\operatorname{artanh} \frac{2\beta_2 (L_{12} - L_1)}{\left(\sqrt{-\Delta_2} - \frac{(2\beta_2 L_{12} + \gamma_2)(2\beta_2 z_0 + \gamma_2)}{\sqrt{-\Delta_2}} \right)} \right) \right) & \forall \Delta_2 < 0 \end{cases} \tag{S.2.23}$$

$$C_{\mathrm{F}3} = \begin{cases} m_3 \cdot \left(\frac{1}{2\beta_3} \ln \frac{P_3(L)}{P_3(L_{12})} + \left(\frac{2}{\sqrt{\Delta_3}} \right) \left(\alpha_3 - \frac{\gamma_3}{2\beta_3} \right) \left(\arctan \frac{2\beta_3 L + \gamma_3}{\sqrt{\Delta_3}} - \arctan \frac{2\beta_3 L_{12} + \gamma_3}{\sqrt{\Delta_3}} \right) \right) & \forall \Delta_3 > 0 \\ m_3 \cdot \left(\frac{1}{2\beta_3} \ln \frac{P_3(L)}{P_3(L_{12})} - \left(\frac{2}{\sqrt{-\Delta_3}} \right) \left(\alpha_3 - \frac{\gamma_3}{2\beta_3} \right) \left(\operatorname{artanh} \frac{2\beta_3 (L - L_{12})}{\left(\sqrt{-\Delta_3} - \frac{(2\beta_3 L + \gamma_3)(2\beta_3 L_{12} + \gamma_3)}{\sqrt{-\Delta_3}} \right)} \right) \right) & \forall \Delta_3 < 0 \end{cases} \tag{S.2.24}$$

Evaluation of $\boldsymbol{\Delta_2}$

To avoid an additional case-by-case analysis for the integration, the discriminants the polynomials $P_2(\xi)$ and $P_3(\xi)$ each were resubsituted to derive that only one of the cases

$$\int \frac{\mathrm{d}\xi}{\beta_i \xi^2 + \gamma_i \xi + \delta_i} \begin{cases} = \frac{2}{\sqrt{\Delta_i}} \cdot \arctan \left(\frac{2\beta_i \xi_i + \gamma_i}{\sqrt{\Delta_i}} \right) & \forall \quad \Delta_i > 0 \\ = -\frac{2}{\sqrt{-\Delta_i}} \cdot \operatorname{artanh} \left(\frac{2\beta_i \xi_i + \gamma_i}{\sqrt{-\Delta_i}} \right) & \forall \quad \Delta_i < 0 \end{cases} \quad [8] \tag{S.2.25}$$

has to be applied for the evaluation of C_F:

$$
\begin{aligned}
\Delta_2 &= 4\beta_2\delta_2 - \gamma_2^2 \\
&= 4 \cdot \left(-\tfrac{\dot{V}_\mathrm{c} m_2}{A_L}\right) \cdot \left(\dot{V}_\mathrm{in} - \tfrac{\dot{V}_\mathrm{c}}{A_L}\left(A_1 - m_2 L_1^2 - 2t_2 L_1\right)\right) - \left(-\tfrac{2\dot{V}_\mathrm{c} t_2}{A_L}\right)^2 \\
&= -4 \cdot \tfrac{\dot{V}_\mathrm{c} m_2 \dot{V}_\mathrm{in}}{A_L} + 4 \cdot \tfrac{\dot{V}_\mathrm{c}^2 m_2 A_1}{A_L^2} - 4 \cdot \tfrac{\dot{V}_\mathrm{c}^2 m_2^2 L_1^2}{A_L^2} - 4 \cdot \tfrac{2\dot{V}_\mathrm{c}^2 m_2 t_2 L_1}{A_L^2} - 4 \cdot \tfrac{\dot{V}_\mathrm{c}^2 t_2^2}{A_L^2} \\
&= \left(4 \cdot \tfrac{\dot{V}_\mathrm{c}^2}{A_L^2}\right) \cdot \left(-m_2 A_1 + m_2^2 L_1^2 - 2m_2 t_2 L_1 - t_2^2\right) - 4 \cdot \tfrac{\dot{V}_\mathrm{c} m_2 \dot{V}_\mathrm{in}}{A_L} \\
&= \left(\tfrac{\dot{V}_\mathrm{c}^2}{A_L^2}\right) \cdot \left(-\tfrac{L_1}{L_2} b_1 b_\Delta - \tfrac{L_1^2}{L_2^2} b_\Delta^2 + 2\tfrac{L_1}{L_2} b_1 b_\Delta + 2\tfrac{L_1^2}{L_2^2} b_\Delta^2 - b_1^2 - 2\tfrac{L_1}{L_2} b_1 b_\Delta - \tfrac{L_1^2}{L_2^2} b_\Delta^2\right) + 2 \cdot \tfrac{b_\Delta \dot{V}_\mathrm{c} \dot{V}_\mathrm{in}}{L_2 A_L} \\
&= \left(\tfrac{\dot{V}_\mathrm{c}^2}{A_L^2}\right) \cdot \left(-\tfrac{L_1}{L_2} b_1 b_\Delta - b_1^2\right) + 2 \cdot \tfrac{b_\Delta \dot{V}_\mathrm{c} \dot{V}_\mathrm{in}}{L_2 A_L} \\
&= \left(\tfrac{\dot{V}_\mathrm{c}}{A_L}\right) \cdot \left(-\tfrac{\dot{V}_\mathrm{c}}{A_L} \tfrac{L_1}{L_2} b_1 b_\Delta - \tfrac{\dot{V}_\mathrm{c}}{A_L} b_1^2 + 2\tfrac{b_\Delta}{L_2} \dot{V}_\mathrm{in}\right) \\
&= \left(\tfrac{\dot{V}_\mathrm{c}}{A_L^2}\right) \left(\dot{V}_\mathrm{in} \cdot \left(2\tfrac{b_\Delta}{L_2} A_L\right) - \dot{V}_\mathrm{c} \cdot \left(\tfrac{L_1}{L_2} b_1 b_\Delta + b_1^2\right)\right) \\
&= \left(\tfrac{\dot{V}_\mathrm{c}}{A_L^2}\right) \left(\dot{V}_\mathrm{in} \cdot \left(2\tfrac{b_\Delta}{L_2} \left(\tfrac{1}{2} b_1 L_1 + \tfrac{1}{2}(b_1 + b_2) L_2 + \tfrac{1}{2} L_3 b_2\right)\right) - \dot{V}_\mathrm{c} \cdot \left(\tfrac{L_1}{L_2} b_1 b_\Delta + b_1^2\right)\right) \\
&= \left(\tfrac{\dot{V}_\mathrm{c}}{A_L^2}\right) \left(\dot{V}_\mathrm{in} \cdot \left(\tfrac{L_1}{L_2} b_\Delta b_1 + b_\Delta b_1 + b_\Delta b_2 + \tfrac{L_3}{L_2} b_2 b_\Delta\right) - \dot{V}_\mathrm{c} \cdot \left(\tfrac{L_1}{L_2} b_1 b_\Delta + b_1^2\right)\right)
\end{aligned}
\tag{S.2.26}
$$

It turns out that the sign of the discriminant cannot be determined exactly without prior knowledge about the parameters and the sign of the discriminants have to be determined “at runtime”.

3 Simplified formulation w^{hyd} and Volume V^{hyd}

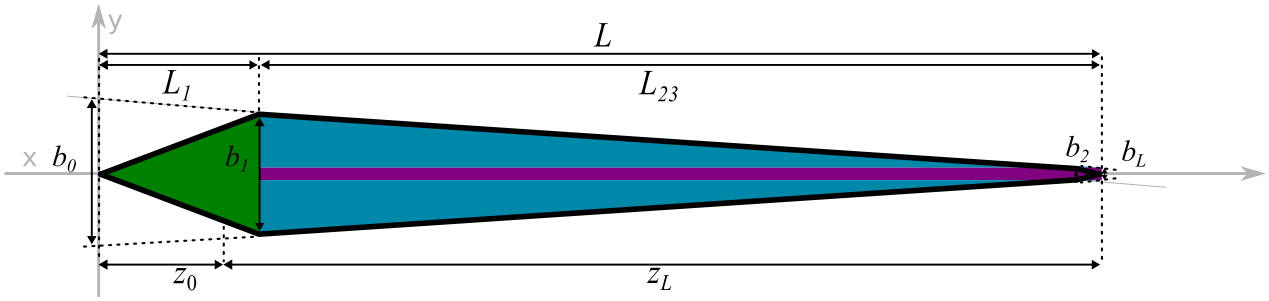

Fig. S.3.1: Total area of an AF4 channel in the simplified model.

A much shorter version has already been derived[6], This model uses the extrapolated channel breadths b_0 and b_L are used. Based on our analytical formulation of $E(x)$, we can reconstruct them easily by

$$b_0 = 2e_2(0) = b_1 + \frac{L_1}{L_2} b_\Delta \tag{S.3.1}$$

and

$$b_L = 2e_2(L) = b_1 + \frac{L_1}{L_2} b_\Delta - \frac{L}{L_2} b_\Delta = b_1 - \frac{L_{23}}{L_2} b_\Delta \quad . \tag{S.3.2}$$

The derivation of a relationship between channel volume and t_{void} is based on Eq. S.2.1. The total membrane area A_L is given by geometrical considerations (Fig. S.3.1) as

$$A_L = \int_0^L b(z)\,\mathrm{d}z = \boxed{\tfrac{1}{2} b_1 L_1} + \boxed{b_L L_{23}} + \boxed{\tfrac{1}{2} b_\Delta L_{23}} \tag{S.3.3}$$

The channel volume in the simplified model is also given by elementary geometry:

$$V^{\text{appgeo}} = w^{\text{appgeo}} A_L \tag{S.3.4}$$

Unfortunately, only the case $z_0 \geqq L_1$ was formulated explicitly[6].

Distal focusing with $z_0 \geqq L_1$

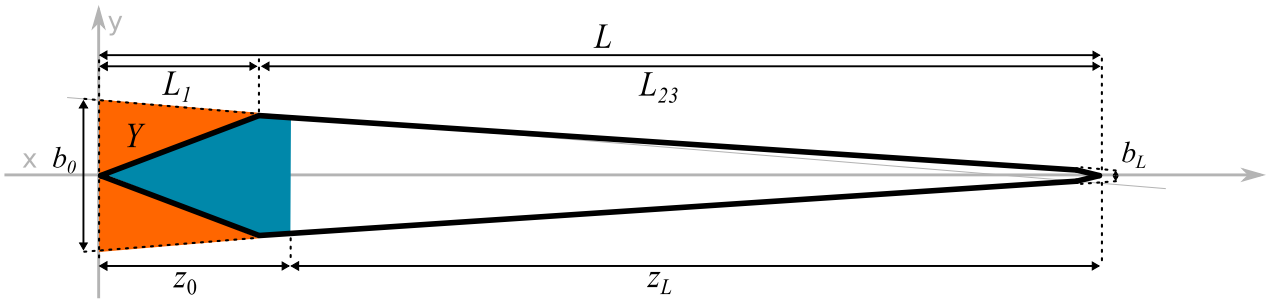

Fig. S.3.2: Simplified model of relevant skipped area sections according to literature[6] in case of a distal focusing point.

$$
\begin{aligned}
t_{\text{void}} &= \frac{V^{\text{appgeo}}}{\dot{V}_{\text{c}}} \ln\left(1 + \frac{\dot{V}_{\text{c}}}{\dot{V}_{\text{e}}}\left(1 - \frac{w\left(b_0 z_0 - \frac{z_0^2(b_0 - b_L)}{2L} - Y\right)}{V^{\text{appgeo}}}\right)\right) \\
&= \frac{V^{\text{appgeo}}}{\dot{V}_{\text{c}}} \ln\left(1 + \frac{\dot{V}_{\text{c}}}{\dot{V}_{\text{e}}}\left(1 - \frac{b_0 z_0 - \frac{z_0^2(b_0 - b_L)}{2L} - Y}{A_L}\right)\right)
\end{aligned}
\tag{S.3.5}
$$

Y is the enclosed area of the elongation from, $e_2(x)$ y-axis and $e_1(x)$ and its symmetrical counterpart (Fig. S.3.2) It can be calculated by simple geometrical considerations as

$$
Y = \frac{1}{2} L_1 b_0 \tag{S.3.6}
$$

Proximal focusing with $z_0 < L_1$

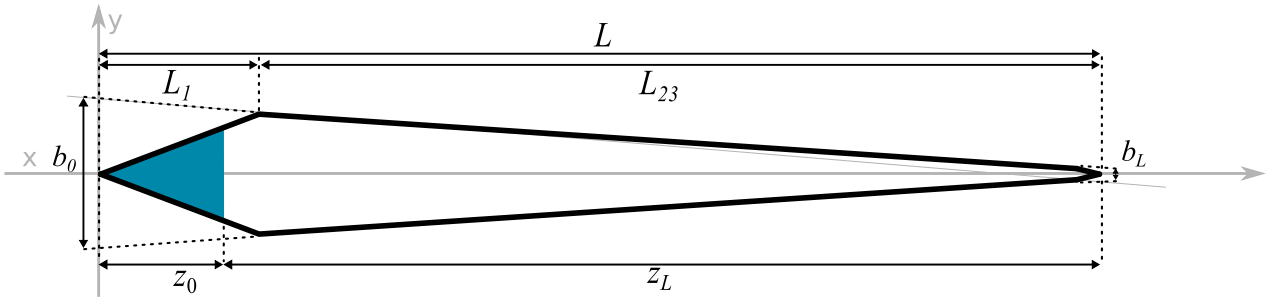

Fig. S.3.3: Simplified model of relevant skipped area sections in case of a proximal focusing point.

In this case, the additional space on the left part has to be considered as well for the skipped area (Fig. S.3.3). This simplifies this skipped part such that it can be expressed as

$$
\begin{aligned}
t_{\text{void}} &= \frac{V^{\text{appgeo}}}{\dot{V}_{\text{c}}} \ln\left(1 + \frac{\dot{V}_{\text{c}}}{\dot{V}_{\text{e}}}\left(1 - \frac{e_1(z_0) \cdot z_0}{A_L}\right)\right) \\
&= \frac{V^{\text{appgeo}}}{\dot{V}_{\text{c}}} \ln\left(1 + \frac{\dot{V}_{\text{c}}}{\dot{V}_{\text{e}}}\left(1 - \frac{\frac{1}{2}\frac{b_1}{L_1} z_0^2}{A_L}\right)\right)
\end{aligned}
\tag{S.3.7}
$$

4 Determination without experimental t_{void}

If a calibration measurement with known diffusion coefficient is used the relationship of R can be formulated as used as well. R_D stands for the dependency of R the calibration

$$
R_D(w) = 6\lambda\left(\coth\left(\frac{1}{2\lambda}\right) - 2\lambda\right) \tag{S.4.1}
$$

$$
\lambda = \frac{DV}{\dot{V}_{\text{c}} w^2} = \frac{DA_L}{\dot{V}_{\text{c}} w} \tag{S.4.2}
$$

In order to eliminate t_{void} as experimental input, eq. S.2.9 is used as a substitution for the retention ratio, resulting in an expression solely dependent on t_{e} and w:

$$
R_{t_{\text{e}}}(w) = \frac{2C_{\text{F}} w}{t_{\text{e}}} \tag{S.4.3}
$$

By adjusting w such that

$$(R_{t_e} - R_D)^2 \rightarrow \min$$

w can be calculated. This corresponds (as an exact solution) to the literature to the "calibration method 5", presented by Wahlund[1] and remains as the only recommended calibration method according to the results presented in the main paper.

5 Detailed description of applied algorithms

Classical Calibration

Inputs:

- void peak t_{void}
- elution time t_{e}
- diffusion coefficient D
- elution flow $\dot{V}_{\text{e}}$
- cross flow $\dot{V}_{\text{c}}$
- relative focus $z_{\%}$;

Outputs:

- channel width w
- channel volume V^0

Constants:

- $w_{\min} \leftarrow 10^{-4}$
- $w_{\max} \leftarrow 10$

Temporary variables:

- measured retention R_{meas}
- variation δ_w
- λ

Calculations:

1 Calculate volume:

$$V^0 \leftarrow \frac{V_c \cdot t_{\text{void}}}{\ln\left(\frac{z_{\%} - (V_e+V_c)/V_c}{1 - (V_E+V_c)/V_c}\right)}$$

2 Calculate R_{meas}:

$$R_{\text{meas}} \leftarrow \frac{t_{\text{void}}}{t_{\text{e}}}$$

3 Initialize w and δ:

$$w \leftarrow \frac{w_{\max} + w_{\min}}{2}$$

$$\delta_w \leftarrow \frac{w_{\max} - w_{\min}}{4}$$

4 Find w such that $|R_{\text{meas}} - R_{\text{calc}}| \stackrel{!}{=} \min$ by bisection:

for $i \leftarrow 0$ to 50 **do**
  $\lambda \leftarrow \frac{D \cdot V^0}{V_C \cdot w^2}$
  $R_{\text{calc}} \leftarrow 6\lambda\left(\frac{1}{\tanh(1/2\lambda)} - 2\lambda\right)$ # $1/\tanh(x) = \coth(x)$
  if $R_{\text{calc}} > R_{\text{meas}}$ **then**
    $w \leftarrow w + \delta_w$
  else
    $w \leftarrow w - \delta_w$
  end if
  $\delta_w \leftarrow \delta_w/2$
end for

Classical Calibration under consideration of the simpiflied trapezoidal shape model

Inputs:

- void peak t_{void}
- elution flow $\dot{V}_{\mathrm{e}}$
- elution time t_{e}
- cross flow $\dot{V}_{\mathrm{c}}$
- diffusion coefficient D
- relative focus $z_{\%}$;
- L_1, L_2, L_3
- b_1, b_2

Outputs:

- channel width w
- channel volume V^{appgeo}

Constants:

- $w_{\mathrm{min}} \leftarrow 10^{-4}$
- $w_{\mathrm{max}} \leftarrow 10$

Temporary variables:

- b_0, b_L
- measured retention R_{meas}
- Channel surface area A_L
- λ
- T_1
- z_0

Calculations:

1 Calculate volume:

$L_{23} \leftarrow L_2 + L_3, \qquad b_\Delta \leftarrow b_1 - b_2$
$A_L \leftarrow \frac{1}{2} b_1 L_1 + b_L L_{23} + \frac{1}{2} b_\Delta L_{23}$
$b_0 \leftarrow b_1 + \frac{L_1}{L_2} b_\Delta$
$b_L \leftarrow b_1 - \frac{L_{23}}{L_2} b_\Delta$
$z_0 \leftarrow z_{\%} L$
if then$(z_0 \geqq L_1)$
  $Y \leftarrow \frac{1}{2} L_1 b_0$
  $\mathrm{T}_1 \leftarrow b_0 z_0 - \frac{z_0^2 (b_0 - b_L)}{2L} - Y$
else
  $\mathrm{T}_1 \leftarrow \frac{1}{2} \frac{b_1}{L_1} z_0^2$
end if
$\mathrm{T}_1 \leftarrow 1 - \frac{\mathrm{T}_1}{A_L}$
$\mathrm{T}_1 \leftarrow \ln\left(1 + \frac{\dot{V}_\mathrm{c}}{\dot{V}_\mathrm{e}} \mathrm{T}_1\right)$
$V^{\mathrm{appgeo}} \leftarrow \frac{\dot{V}_\mathrm{c} t_{\mathrm{void}}}{\mathrm{T}_1}$

2 Calculate R_{meas}:

$$R_{\mathrm{meas}} \leftarrow \frac{t_{\mathrm{void}}}{t_\mathrm{e}}$$

3 Initialize w and δ:

$$w \leftarrow \frac{w_{\max} + w_{\min}}{2}$$
$$\delta_w \leftarrow \frac{w_{\max} - w_{\min}}{4}$$

4 Find w such that $|R_{\mathrm{meas}} - R_{\mathrm{calc}}| \stackrel{!}{=} \min$ by bisection:

for $i \leftarrow 0$ to 50 **do**
  $\lambda \leftarrow \frac{D \cdot V^{\mathrm{appgeo}}}{V_C \cdot w^2}$
  $R_{\mathrm{calc}} \leftarrow 6\lambda \left(\frac{1}{\tanh(1/2\lambda)} - 2\lambda\right)$ # $1/\tanh(x) = \coth(x)$
  if $R_{\mathrm{calc}} > R_{\mathrm{meas}}$ **then**
    $w \leftarrow w + \delta_w$
  else
    $w \leftarrow w - \delta_w$
  end if
  $\delta_w \leftarrow \delta_w / 2$
end for

Calibration of channel height by V^{geo}

Inputs:

- void peak t_{void}
- elution time t_{e}
- cross flow $\dot{V}_{\text{c}}$
- diffusion coefficient D
- L_1, L_2, L_3
- b_1, b_L

Outputs:

- channel height w
- channel volume V^{geo}

Temporary variables:

- measured retention R_{meas}
- calculated retention R_{calc}
- variation δ_λ
- λ
- S
- L_{12}, L
- m_1, m_2
- t_2
- A_L
- A_3

Constants:

- $\lambda_{\min} \leftarrow 10^{-5}$
- $\lambda_{\max} \leftarrow 100$

Calculations:

1 Calculate R_{meas}:

$$R_{\text{meas}} \leftarrow \frac{t_{\text{void}}}{t_{\text{e}}}$$

2 Initialize λ and δ_λ:

$$\lambda \leftarrow \frac{\lambda_{\min} + \lambda_{\max}}{2}$$

$$\delta_\lambda \leftarrow \frac{\lambda_{\max} - \lambda_{\min}}{4}$$

3 Find λ such that $|R_{\text{meas}} - R_{\text{calc}}| \stackrel{!}{=} \min$ by bisection:

for $i \leftarrow 0$ to 50 **do**
  $R_{\text{calc}} \leftarrow 6\lambda \left(\frac{1}{\tanh(1/2\lambda)} - 2\lambda \right)$ # $1/\tanh(x) = \coth(x)$
  if $R_{\text{calc}} > R_{\text{meas}}$ **then**
    $\lambda \leftarrow \lambda + \delta_\lambda$
  else
    $\lambda \leftarrow \lambda - \delta_\lambda$
  end if
  $\delta_\lambda \leftarrow \delta_\lambda / 2$
end for

4 Calculate substitution term S:

$$S \leftarrow \frac{\lambda \cdot \dot{V}_{\text{c}}}{D}$$

5 Calculate membrane area A_L:

$A_1 \leftarrow \frac{1}{2} b_1 L_1 \qquad A_2 \leftarrow \frac{1}{2}(b_1 + b_2) L_2 \qquad A_3 \leftarrow \frac{1}{2} L_3 b_2$

$A_L \leftarrow A_1 + A_2 + A_3$

6 Calculate w:

$$w \leftarrow \frac{A_L}{S}$$

7 Calculate V^{geo}:

$$V^{\text{geo}} \leftarrow A_L \cdot w$$

Calibration of channel height by V^{hyd}

Inputs:

- void peak t_{void}
- elution flow $\dot{V}_{\text{e}}$
- cross flow $\dot{V}_{\text{c}}$
- relative focus $z_{\%}$;
- L_1, L_2, L_3
- b_1, b_2

Outputs:

- channel width w
- channel volume V^{hyd}

Temporary variables:

- z_0
- $\dot{V}_{\text{in}}$
- L_{12}, L
- b_Δ
- m_1, m_2, m_3
- t_2, t_3
- $C_{\text{F1}}, C_{\text{F2}}, C_{\text{F3}}, C_{\text{F}}$
- T_1, T_2

Calculations:

1 Calculate "derived" parameters:

$L_{12} \leftarrow L_1 + L_2 \qquad L \leftarrow L_{12} + L_3 \qquad z_0 \leftarrow z_{\%} \cdot L \qquad b_\Delta \leftarrow b_1 - b_2 \qquad \dot{V}_{\text{in}} \leftarrow \dot{V}_{\text{e}} + \dot{V}_{\text{c}}$

2 Calculate slopes and offsets of the border lines of the channel plain:

$m_1 \leftarrow \frac{b_1}{2L_1} \qquad m_2 \leftarrow -\frac{b_\Delta}{2L_2} \qquad m_3 \leftarrow -\frac{b_2}{2L_3}$

$t_2 \leftarrow \frac{1}{2}\left(b_1 + \frac{L_1}{L_2} b_\Delta\right) \qquad t_3 \leftarrow \frac{Lb_2}{2L_3}$

3 Calculate area sections of the channel plain:

$A_1 \leftarrow \frac{1}{2} b_1 L_1 \qquad A_2 \leftarrow \frac{1}{2}(b_1 + b_2) L_2 \qquad A_3 \leftarrow \frac{1}{2} L_3 b_2$

$A_L \leftarrow A_1 + A_2 + A_3$

4 Simple numerical integration via Riemann sum (see subroutines):

$C_{\text{F}} \leftarrow \text{calcCF}(.....)$

5 Calculate w:

$w \leftarrow \frac{t_{\text{void}}}{2 \cdot C_{\text{F}}}$

6 Calculate V^{hyd}:

$V^{\text{hyd}} \leftarrow A_L \cdot w$

S subroutines

S1 calcCF

initialize ξnear z_0 on the ξ-grid
$\Delta\xi \leftarrow \frac{L}{n}$
$\xi < z_0$
while $\xi < z_0$ **do**
  $\xi \leftarrow \xi + \Delta\xi$
end while

# Calculate $C_{\mathrm{F}1}$
while $\xi < z_0$ **do**
  $A_\xi \leftarrow m_1 \xi^2$
  $\dot{V}_\xi \leftarrow \dot{V}_{\mathrm{in}} - \dot{V}_{\mathrm{c}} \frac{A_\xi}{A_L}$
  $E_{\dot{V}\xi} \leftarrow \frac{m_1 \xi}{\dot{V}_\xi}$
  $C_{\mathrm{F}}1 \leftarrow C_{\mathrm{F}}1 + E_{\dot{V}\xi} \Delta\xi$
  $\xi \leftarrow \xi + \Delta\xi$
end while

# Calculate $C_{\mathrm{F}2}$
while $\xi < L_{12}$ **do**
  $A_\xi \leftarrow A_1 + m_2 \left(\xi^2 - L_1^2\right) + 2t_2 \left(\xi - L_1\right)$
  $\dot{V}_\xi \leftarrow \dot{V}_{\mathrm{in}} - \dot{V}_{\mathrm{c}} \frac{A_\xi}{A_L}$
  $E_{\dot{V}\xi} \leftarrow \frac{m_2 \xi + t_2}{\dot{V}_\xi}$
  $C_{\mathrm{F}}2 \leftarrow C_{\mathrm{F}}2 + E_{\dot{V}\xi} \Delta\xi$
  $\xi \leftarrow \xi + \Delta\xi$
end while

# Calculate $C_{\mathrm{F}3}$
while $\xi < L$ **do**
  $A_\xi \leftarrow A_1 + A_2 + m_3 \left(\xi^2 - L_{12}^2\right) + 2t_3 \left(\xi - L_{12}\right)$
  $\dot{V}_\xi \leftarrow \dot{V}_{\mathrm{in}} - \dot{V}_{\mathrm{c}} \frac{A_\xi}{A_L}$
  $E_{\dot{V}\xi} \leftarrow \frac{m_3 \xi + t_3}{\dot{V}_\xi}$
  $C_{\mathrm{F}}3 \leftarrow C_{\mathrm{F}}3 + E_{\dot{V}\xi} \Delta\xi$
  $\xi \leftarrow \xi + \Delta\xi$
end while

General formulation of numerical C_{F} integration for arbitrary channel shapes

The simple integration procedure above for three channel sections could also be generalized by the following when the channel shape is provided as a set of functions $e_s(x)$:

for $s \leftarrow 1$ to S **do**
  while $\xi < L$ **do**
    $A_\xi \leftarrow \sum_{\sigma=1}^{s} A_\sigma + \int_{L1s}^{\xi} e_s(x)\,\mathrm{d}x$
    $\dot{V}_\xi \leftarrow \dot{V}_{\mathrm{in}} - \dot{V}_{\mathrm{c}} \frac{A_\xi}{A_L}$
    $E_{\dot{V}\xi} \leftarrow \frac{e_s(\xi)}{\dot{V}_\xi}$
    $C_{\mathrm{F}} \leftarrow C_{\mathrm{F}} + E_{\dot{V}\xi} \Delta\xi$
    $\xi \leftarrow \xi + \Delta\xi$
  end while
end for

Alternatively, the Riemann sum could be exchanged by a trapezoidal rule approach.

Calibration of channel height by V^{noT}

Inputs:

- void peak t_{void}
- elution flow $\dot{V}_{\mathrm{e}}$
- cross flow $\dot{V}_{\mathrm{c}}$
- relative focus $z_{\%}$
- L_1, L_2, L_3
- b_1, b_2

Outputs:

- channel width w
- channel volume V^{noT}

Temporary variables:

- z_0
- $\dot{V}_{\mathrm{in}}$
- L_{12}, L
- b_Δ
- m_1, m_2, m_3
- t_2, t_3
- $C_{\mathrm{F1}}, C_{\mathrm{F2}}, C_{\mathrm{F3}}, C_{\mathrm{F}}$

Calculations:

1 Calculate "derived" parameters:

$L_{12} \leftarrow L_1 + L_2 \qquad L \leftarrow L_{12} + L_3 \qquad z_0 \leftarrow z_{\%} \cdot L \qquad b_\Delta \leftarrow b_1 - b_2 \qquad \dot{V}_{\mathrm{in}} \leftarrow \dot{V}_{\mathrm{e}} + \dot{V}_{\mathrm{c}}$

2 Calculate slopes and offsets of the border lines of the channel plain:

$m_1 \leftarrow \frac{b_1}{2L_1} \qquad m_2 \leftarrow -\frac{b_\Delta}{2L_2} \qquad m_3 \leftarrow -\frac{b_2}{2L_3}$

$t_2 \leftarrow \frac{1}{2}\left(b_1 + \frac{L_1}{L_2} b_\Delta\right) \qquad t_3 \leftarrow \frac{L b_2}{2L_3}$

3 Calculate area sections of the channel plain:

$A_1 \leftarrow \frac{1}{2} b_1 L_1 \qquad A_2 \leftarrow \frac{1}{2}(b_1 + b_2) L_2 \qquad A_3 \leftarrow \frac{1}{2} L_3 b_2$

$A_L \leftarrow A_1 + A_2 + A_3$

4 Numerical integration for C_{F} via Riemann sum (see subroutine **S1** of V^{noT} above):

$C_{\mathrm{F}} \leftarrow \mathrm{calcCF}(.....)$

5 Calculate w by minimizing $\Delta^2 = (R_{t_e} - R_D)^2$:

Initialize:
$w_\mathrm{L} \leftarrow 1, w_\mathrm{R} \leftarrow 1000, w_\mathrm{M} \leftarrow \frac{w_\mathrm{L}+w_\mathrm{R}}{2}$
$\Delta_{w_\mathrm{L}} \leftarrow \mathrm{RDiff}(\Delta_{w_\mathrm{L}}), \Delta_{w_\mathrm{R}} \leftarrow \mathrm{RDiff}(\Delta_{w_\mathrm{R}}), \Delta_{w_\mathrm{M}} \leftarrow \mathrm{RDiff}(\Delta_{w_\mathrm{M}})$
while conv $< 10^{-8}$ **do**
  if $\Delta_{w_\mathrm{L}} > \Delta_{w_\mathrm{M}}$ and $\Delta_{w_\mathrm{M}} > \Delta_{w_\mathrm{R}}$ **then** # "Leap" right along gradient descent
    $w_\mathrm{L} \leftarrow w_\mathrm{M}, \Delta_{w_\mathrm{L}} \leftarrow \Delta_{w_\mathrm{M}}$
    $w_\mathrm{M} \leftarrow w_\mathrm{R}, \Delta_{w_\mathrm{M}} \leftarrow \Delta_{w_\mathrm{R}}$
    $w_\mathrm{R} \leftarrow w_\mathrm{R} + |w_\mathrm{L} - w_\mathrm{M}|$
    $\Delta_{w_\mathrm{R}} \leftarrow \mathrm{RDiff}(w_\mathrm{R})$
  else if $\Delta_{w_\mathrm{L}} < \Delta_{w_\mathrm{M}}$ and $\Delta_{w_\mathrm{M}} < \Delta_{w_\mathrm{R}}$ **then** #"Leap" left along gradient descent
    $w_\mathrm{R} \leftarrow w_\mathrm{M}, \Delta_{w_\mathrm{R}} \leftarrow \Delta_{w_\mathrm{M}}$
    $w_\mathrm{M} \leftarrow w_\mathrm{L}, \Delta_{w_\mathrm{M}} \leftarrow \Delta_{w_\mathrm{L}}$
    $w_\mathrm{L} \leftarrow w_\mathrm{L} - |w_\mathrm{R} - w_\mathrm{M}|$
    $\Delta_{w_\mathrm{L}} \leftarrow \mathrm{RDiff}(w_\mathrm{L})$
  else if $\Delta_{w_\mathrm{L}} > \Delta_{w_\mathrm{M}}$ and $\Delta_{w_\mathrm{M}} < \Delta_{w_\mathrm{R}}$ **then** #Shrink both distances about half
    $w_\mathrm{L} \leftarrow \frac{w_\mathrm{L}+w_\mathrm{M}}{2}, \Delta_{w_\mathrm{L}} \leftarrow \mathrm{RDiff}(w_\mathrm{L})$
    $w_\mathrm{R} \leftarrow \frac{w_\mathrm{R}+w_\mathrm{M}}{2}, \Delta_{w_\mathrm{R}} \leftarrow \mathrm{RDiff}(w_\mathrm{R})$
  end if
end while

S subroutines

S2 RDiff

calculate $\Delta = (R_{t_e} - R_D)^2$:
  $R_{t_e} \leftarrow \frac{2C_\mathrm{F} w}{t_e}$
  $\lambda \leftarrow \frac{DA_z}{V_c w}$
  $R_D \leftarrow 6\lambda\,(-2\lambda)$
  return $(R_{t_e} - R_D)^2$

6 Complete data sets

Measured raw data

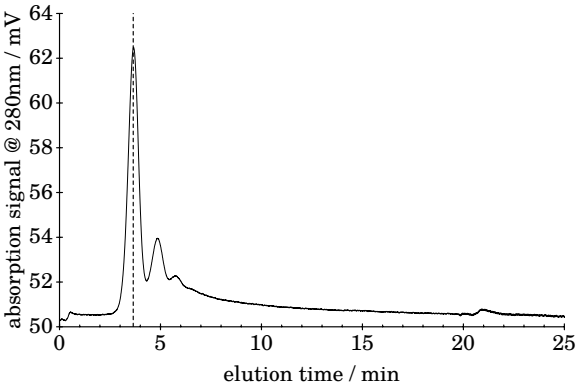

(a) Position of t_e, replicate 1.

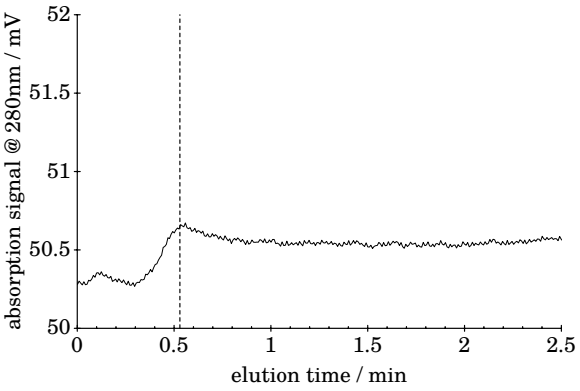

(b) Detailed starting section of fractogram S.6.1a; Position of t_{void}, replicate 1.

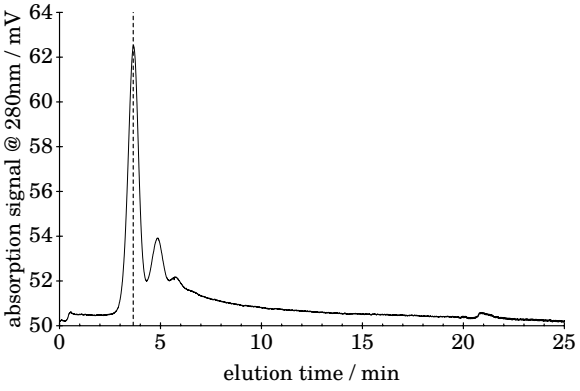

(c) Position of t_e, replicate 2.

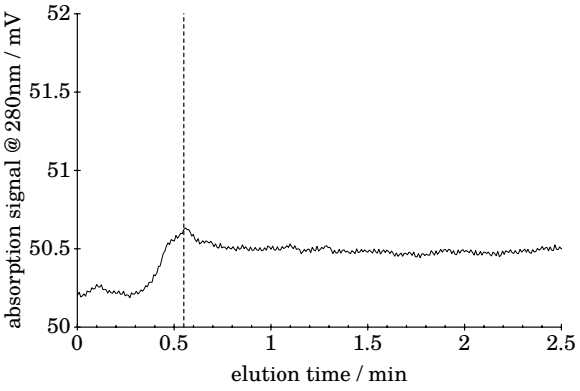

(d) Detailed starting section of fractogram S.6.1c; Position of t_{void}, replicate 2.

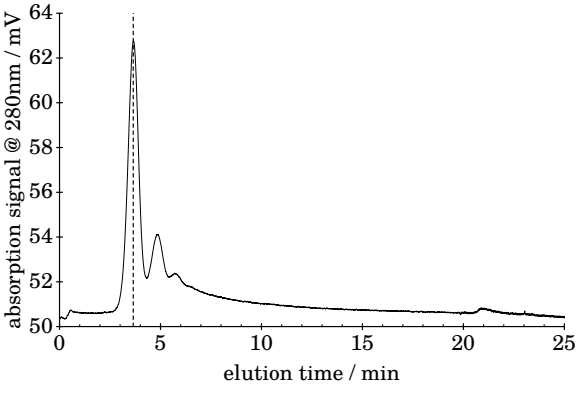

(e) Position of t_e, replicate 3.

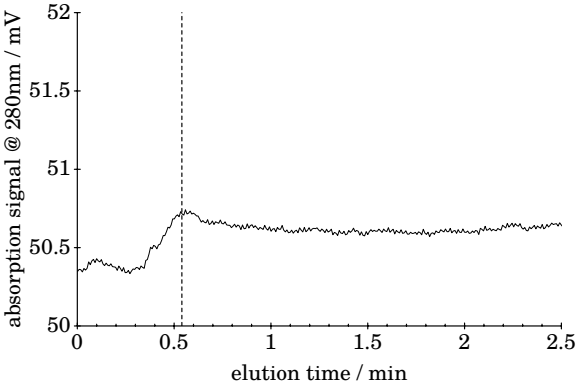

(f) Detailed starting section of fractogram S.6.1e; Position of t_{void}, replicate 3.

Fig. S.6.1: Raw fractograms of BSA measurements at $\dot{V}_c = 2.5\,^{\mathrm{ml}}/_{\mathrm{min}}$

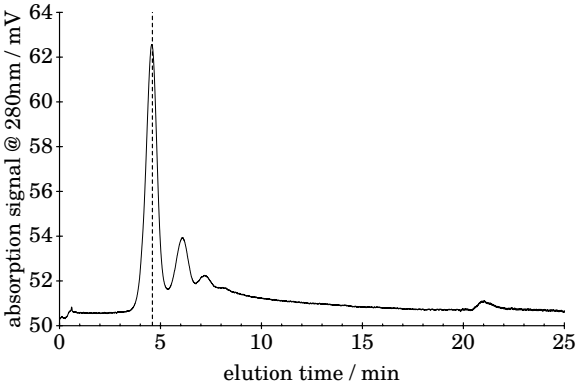

(a) Position of t_e, replicate 1.

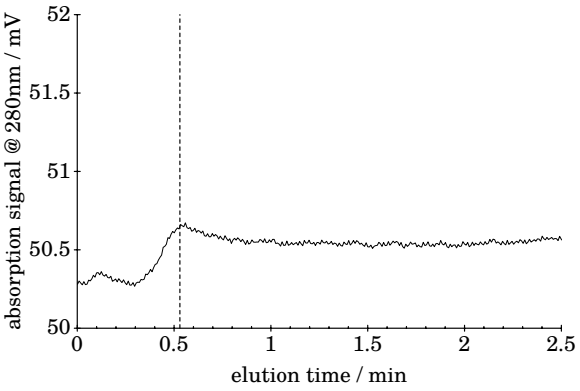

(b) Detailed starting section of fractogram S.6.2a; Position of t_{void}, replicate 1.

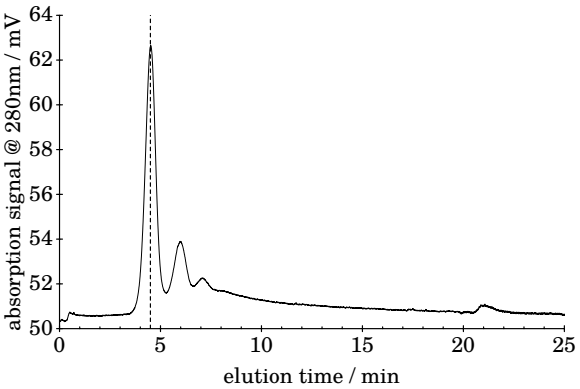

(c) Position of t_e, replicate 2.

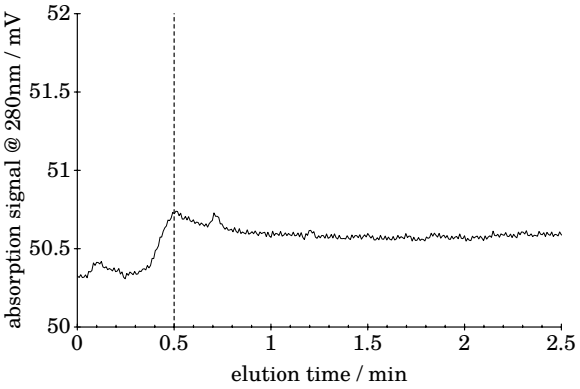

(d) Detailed starting section of fractogram S.6.2c; Position of t_{void}, replicate 2.

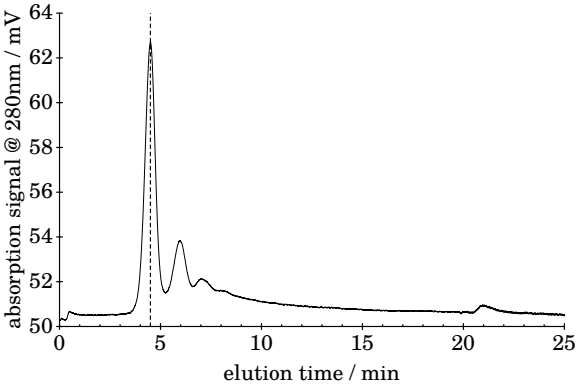

(e) Position of t_e, replicate 3.

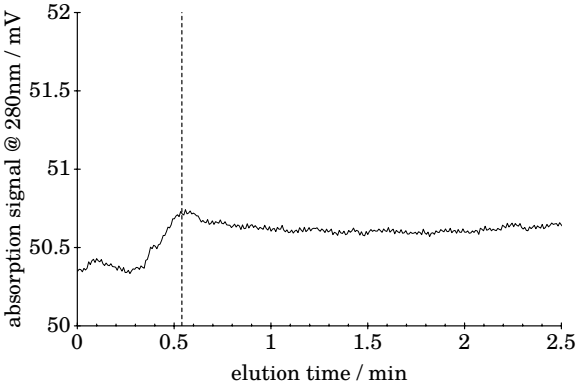

(f) Detailed starting section of fractogram S.6.2e; Position of t_{void}, replicate 3.

Fig. S.6.2: Raw fractograms of BSA measurements at $\dot{V}_c = 3.5 {}^{\mathrm{ml}}/_{\mathrm{min}}$

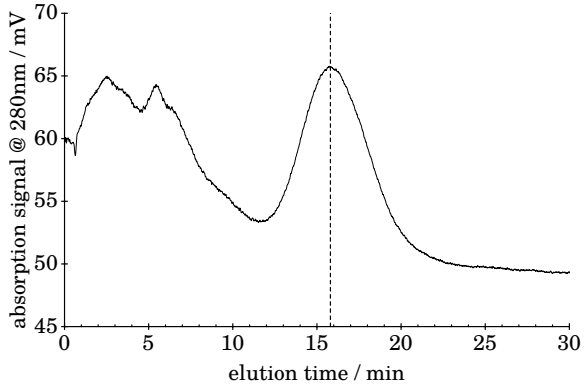

(a) Position of t_e with UV detection signal

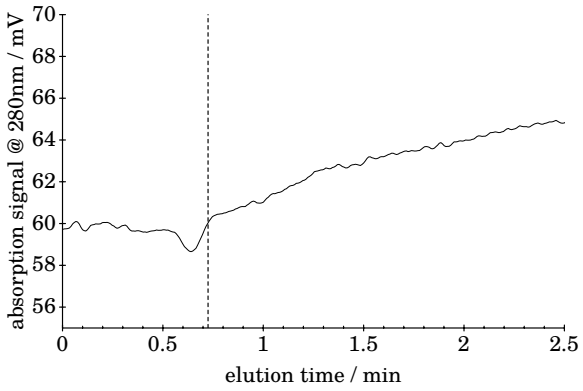

(b) Detailed starting section of fractogram S.6.3a with UV detection signal and position of t_{void}.

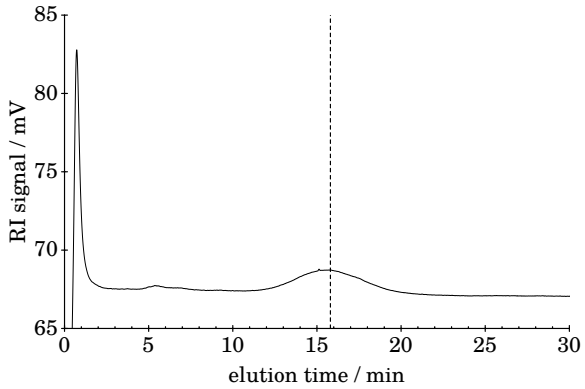

(c) Position of t_e with RI detection signal

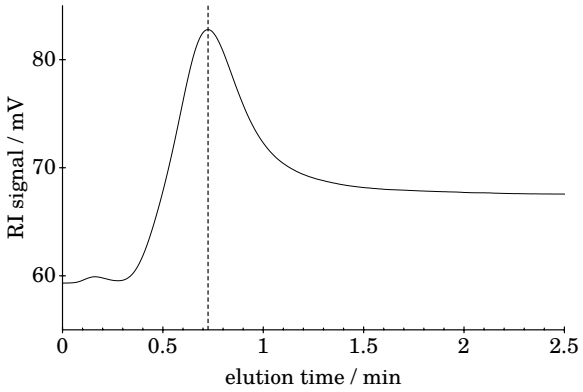

(d) Detailed starting section of fractogram S.6.3c with RI detection signal and position of t_{void}.

Fig. S.6.3: Raw fractograms of PS measurements at $\dot{V}_c = 0.5\,^{ml}/_{min}$, replicate 1.

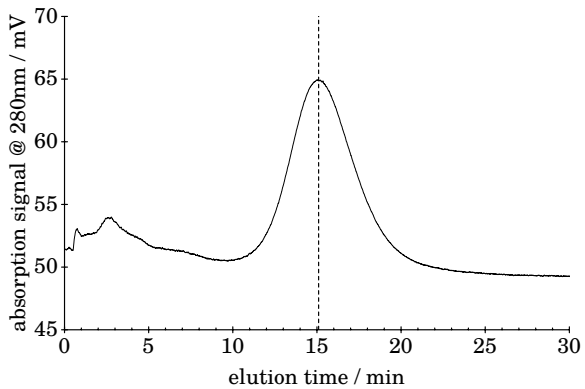

(a) Position of t_e with UV detection signal

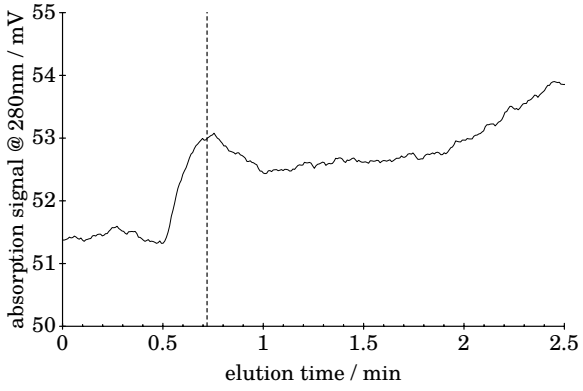

(b) Detailed starting section of fractogram S.6.5a with UV detection signal and position of t_{void}.

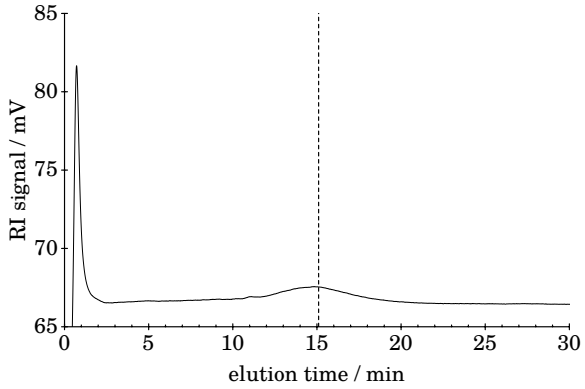

(c) Position of t_e with RI detection signal

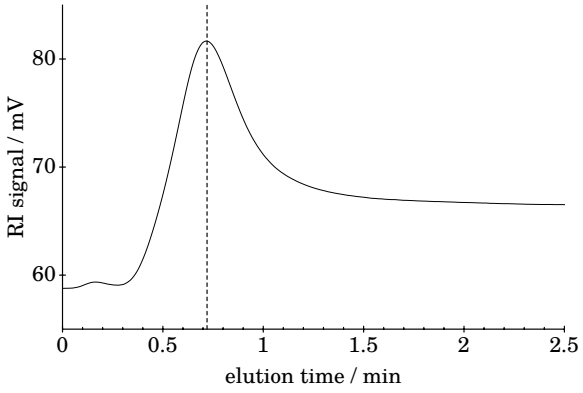

(d) Detailed starting section of fractogram S.6.5c with RI detection signal and position of t_{void}.

Fig. S.6.5: Raw fractograms of PS measurements at $\dot{V}_c = 0.5\,^{ml}/_{min}$, replicate 3.

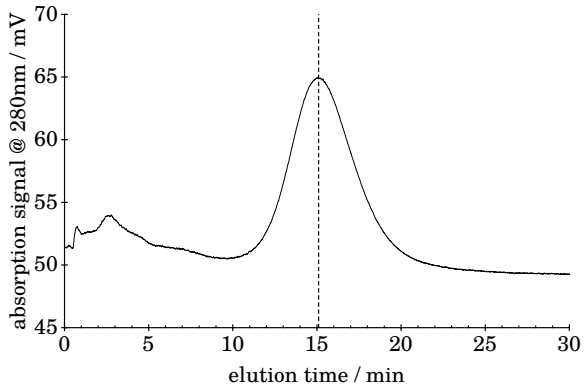

(a) Position of t_e with UV detection signal

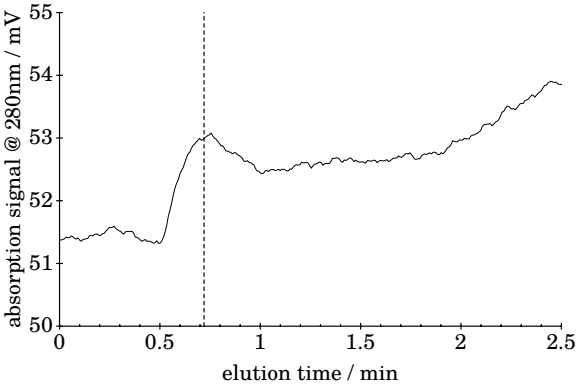

(b) Detailed starting section of fractogram S.6.4a with UV detection signal and position of t_{void}.

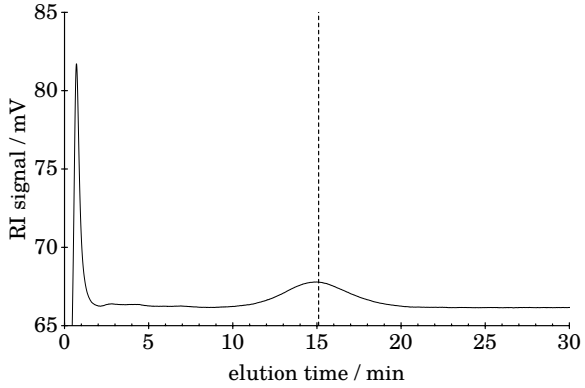

(c) Position of t_e with RI detection signal

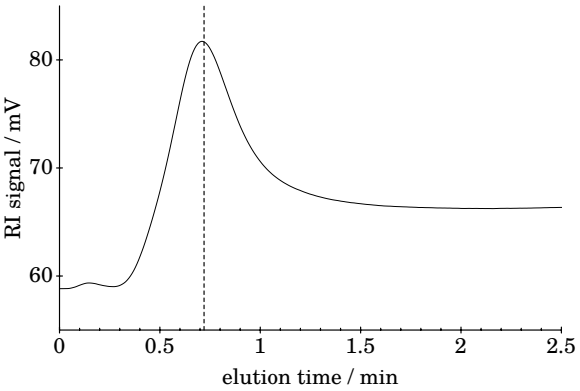

(d) Detailed starting section of fractogram S.6.4c with RI detection signal and position of t_{void}.

Fig. S.6.4: Raw fractograms of PS measurements at $\dot{V}_c = 0.5\,^{ml}/_{min}$, replicate 2.

Evaluated of own calibration experiments with BSA and PS for different $z_{\%}$

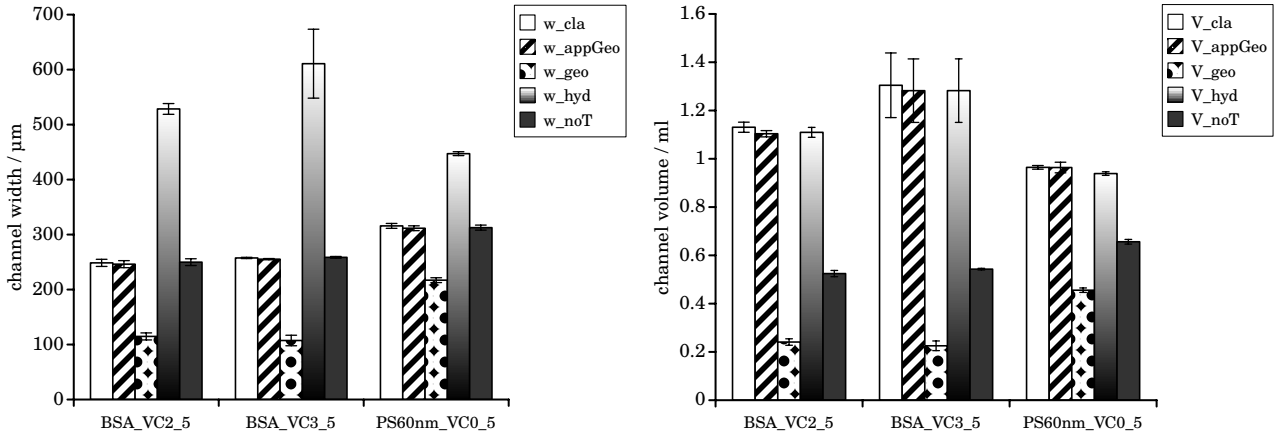

(a) Calibration results for w (b) Calibration results for V

Fig. S.6.6: Statistical results of w and V from all 5 calibration algorithms for assumed $z_{\%} = 8\,\%$

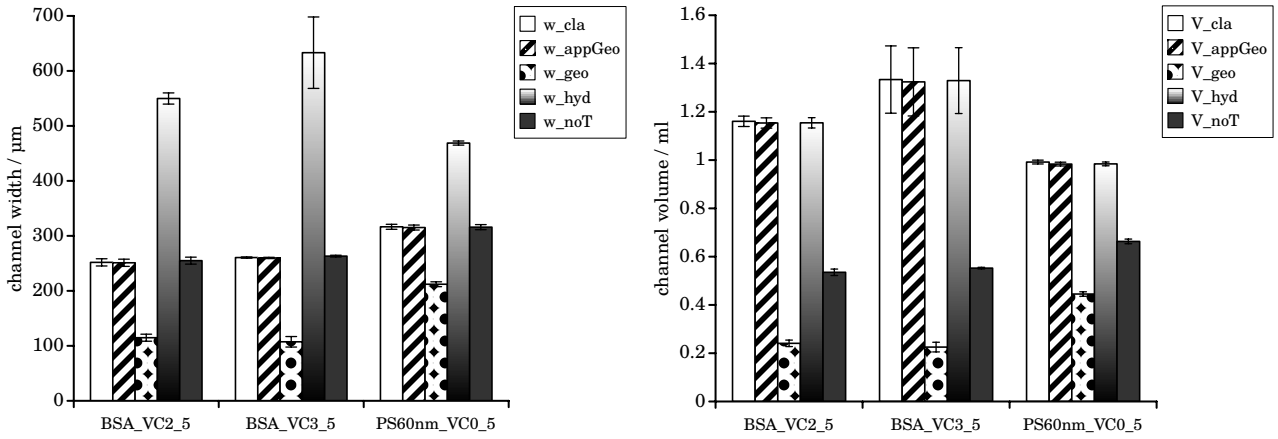

(a) Calibration results for w (b) Calibration results for V

Fig. S.6.7: Statistical results of w and V from all 5 calibration algorithms for assumed $z_{\%} = 12\,\%$

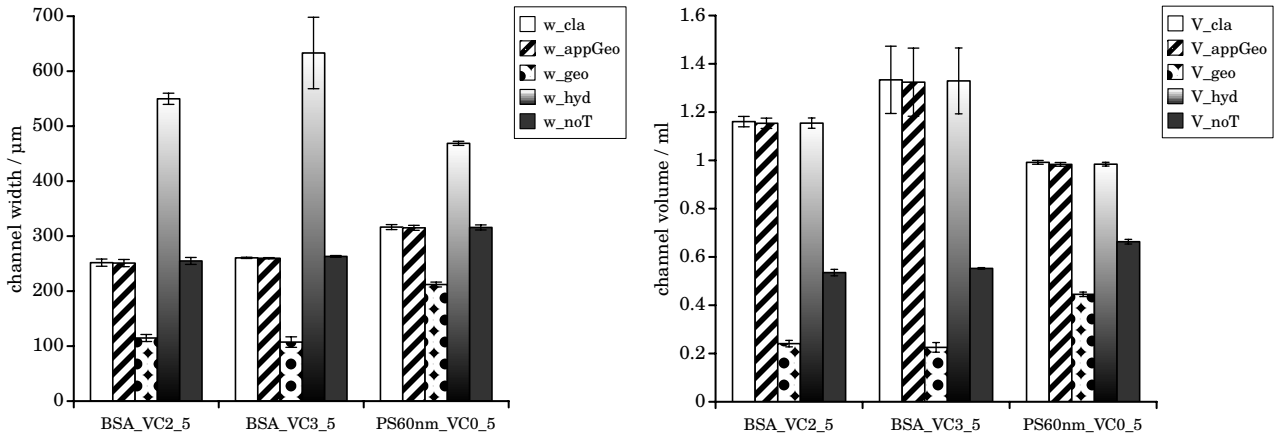

(a) Calibration results for w (b) Calibration results for V

Fig. S.6.8: Statistical results of w and V from all 5 calibration algorithms for assumed $z_{\%} = 16\,\%$

Single results of own calibration experiments with BSA and PS, $z_{\%} = 8\,\%$

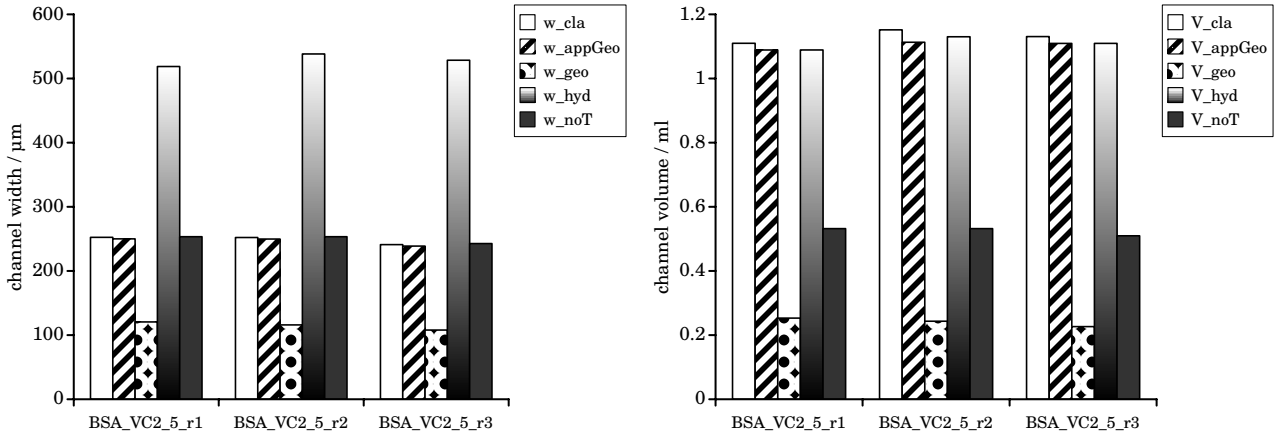

(a) Calibration results for w (b) Calibration results for V

Fig. S.6.9: Results of w and V from all 5 calibration algorithms for BSA measurements at $\dot{V}_c = 2.5\,^{\mathrm{ml}}/_{\mathrm{min}}$, $z_{\%} = 8\,\%$

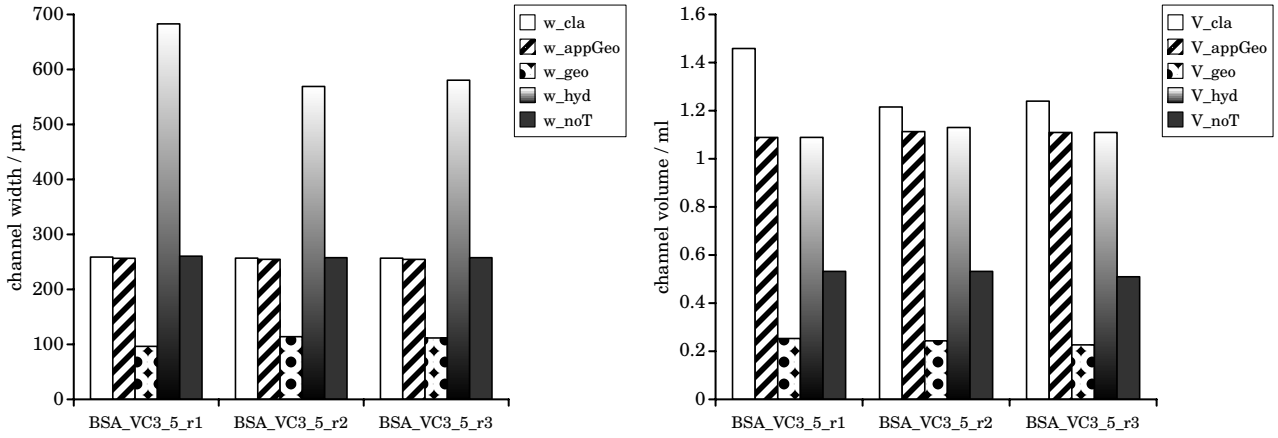

(a) Calibration results for w (b) Calibration results for V

Fig. S.6.10: Results of w and V from all 5 calibration algorithms for BSA measurements at $\dot{V}_c = 3.5\,^{\mathrm{ml}}/_{\mathrm{min}}$, $z_{\%} = 8\,\%$

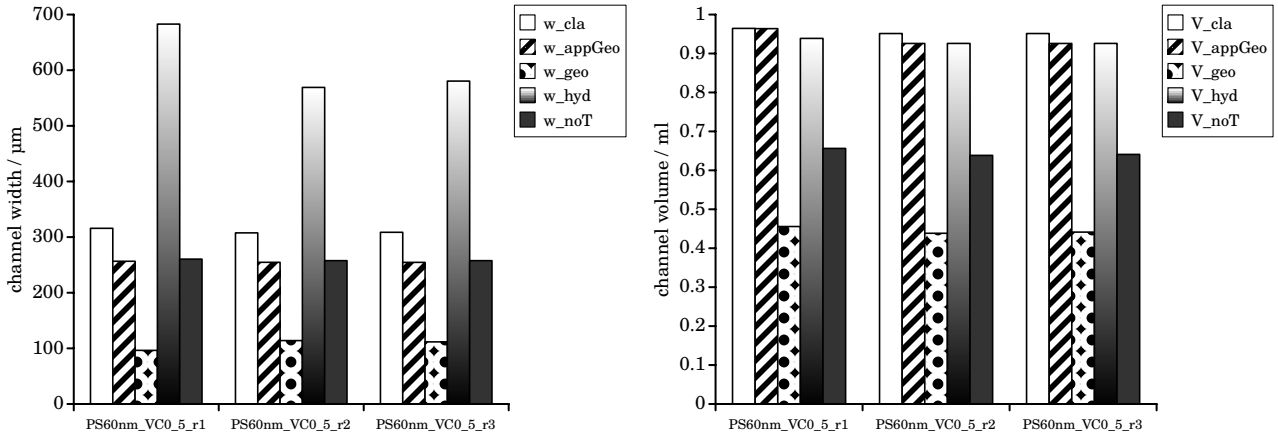

(a) Calibration results for w (b) Calibration results for V

Fig. S.6.11: Results of w and V from all 5 calibration algorithms for PS measurements at $\dot{V}_c = 0.5\,^{\mathrm{ml}}/_{\mathrm{min}}$, $z_{\%} = 8\,\%$

Single results of own calibration experiments with BSA and PS, $z_{\%} = 12\,\%$

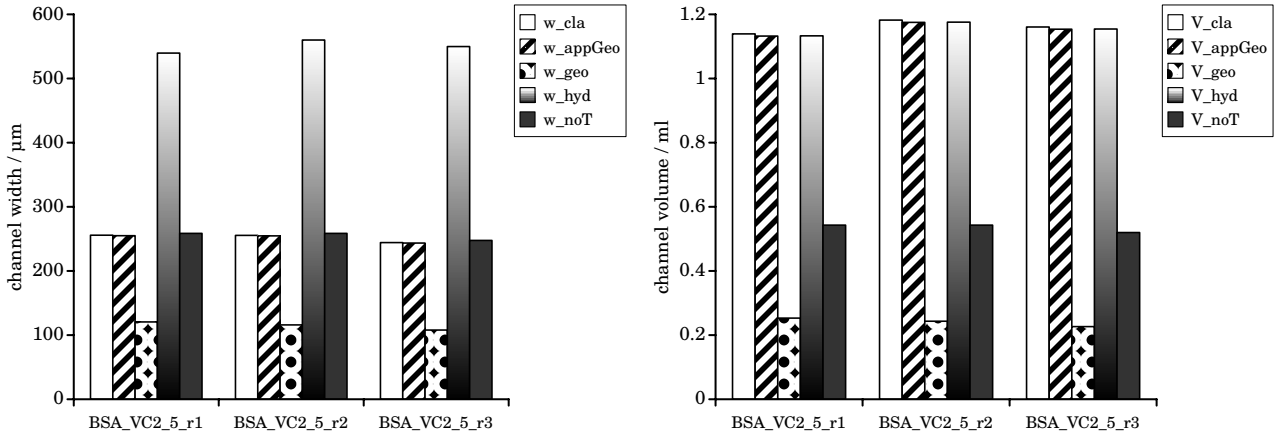

(a) Calibration results for w (b) Calibration results for V

Fig. S.6.12: Results of w and V from all 5 calibration algorithms for BSA measurements at $\dot{V}_c = 2.5\,^{\mathrm{ml}}/_{\mathrm{min}}$, $z_{\%} = 12\,\%$

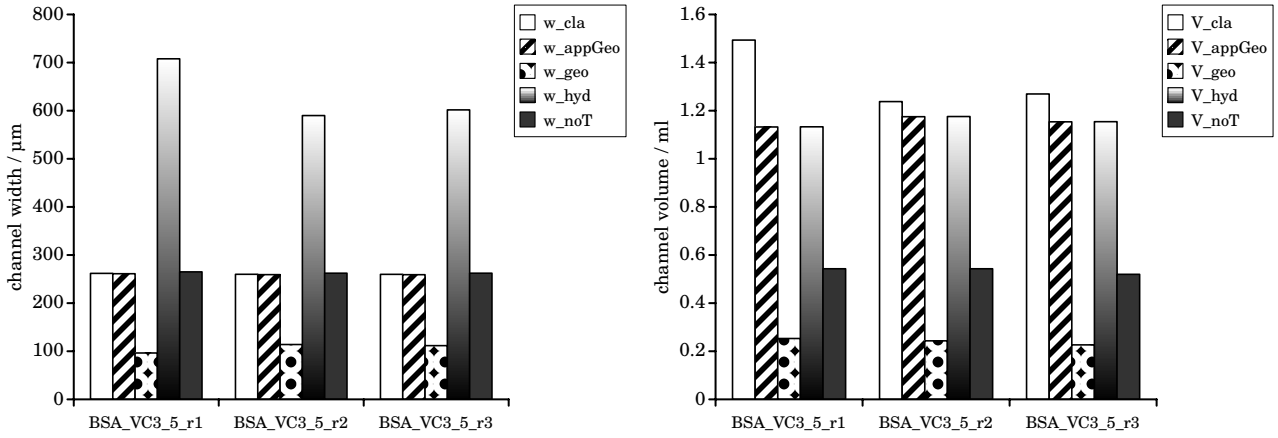

(a) Calibration results for w (b) Calibration results for V

Fig. S.6.13: Results of w and V from all 5 calibration algorithms for BSA measurements at $\dot{V}_c = 3.5\,^{\mathrm{ml}}/_{\mathrm{min}}$, $z_{\%} = 12\,\%$

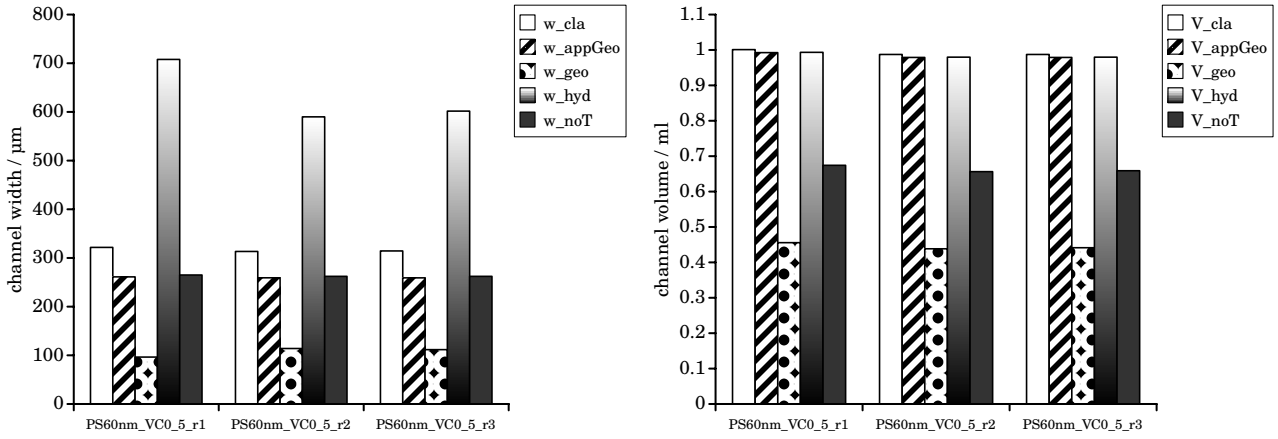

(a) Calibration results for w (b) Calibration results for V

Fig. S.6.14: Results of w and V from all 5 calibration algorithms for PS measurements at $\dot{V}_c = 0.5\,^{\mathrm{ml}}/_{\mathrm{min}}$, $z_{\%} = 12\,\%$

Single results of own calibration experiments with BSA and PS, $z_{\%} = 16\,\%$

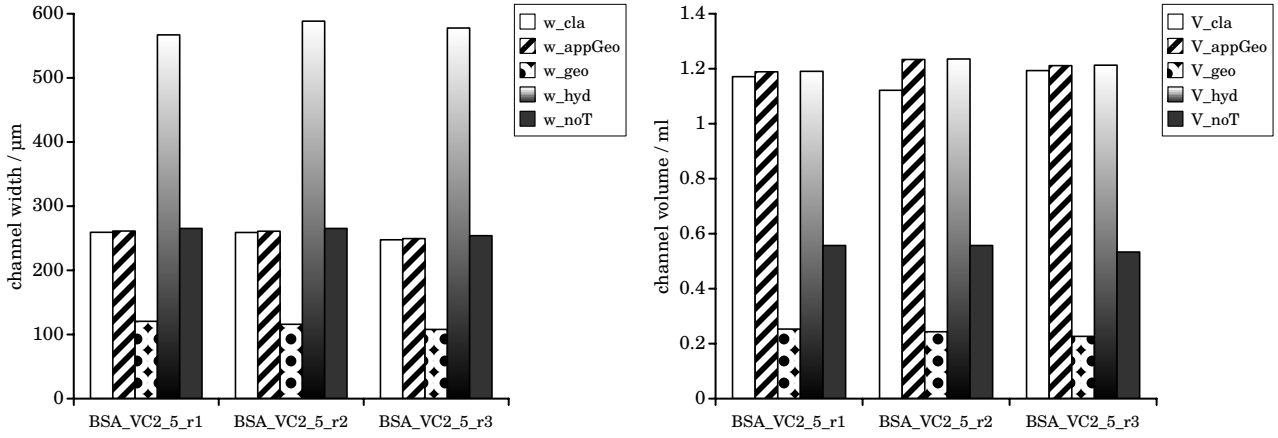

(a) Calibration results for w (b) Calibration results for V

Fig. S.6.15: Results of w and V from all 5 calibration algorithms for BSA measurements at $\dot{V}_c = 2.5\,^{\mathrm{ml}}/_{\mathrm{min}}$, $z_{\%} = 16\,\%$

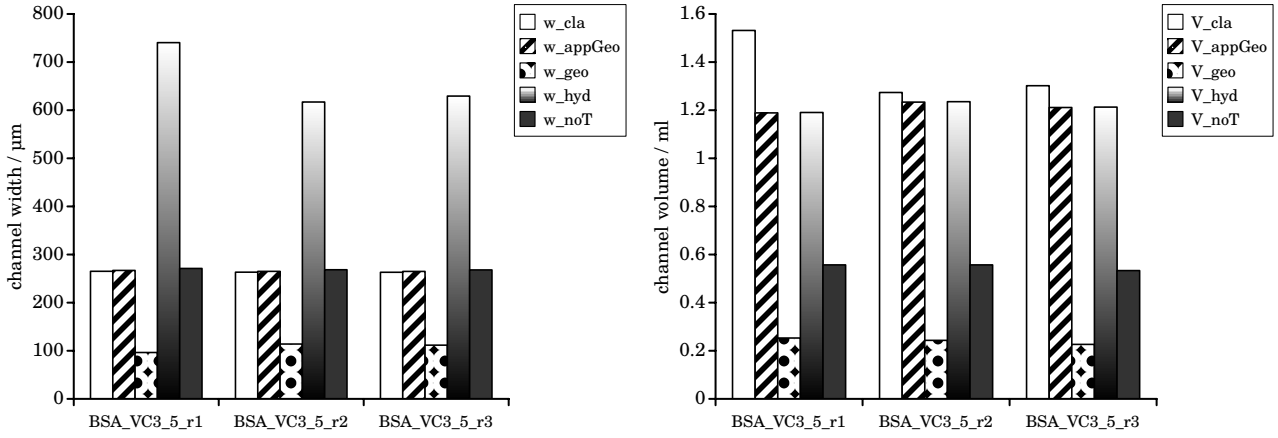

(a) Calibration results for w (b) Calibration results for V

Fig. S.6.16: Results of w and V from all 5 calibration algorithms for BSA measurements at $\dot{V}_c = 3.5\,^{\mathrm{ml}}/_{\mathrm{min}}$, $z_{\%} = 16\,\%$

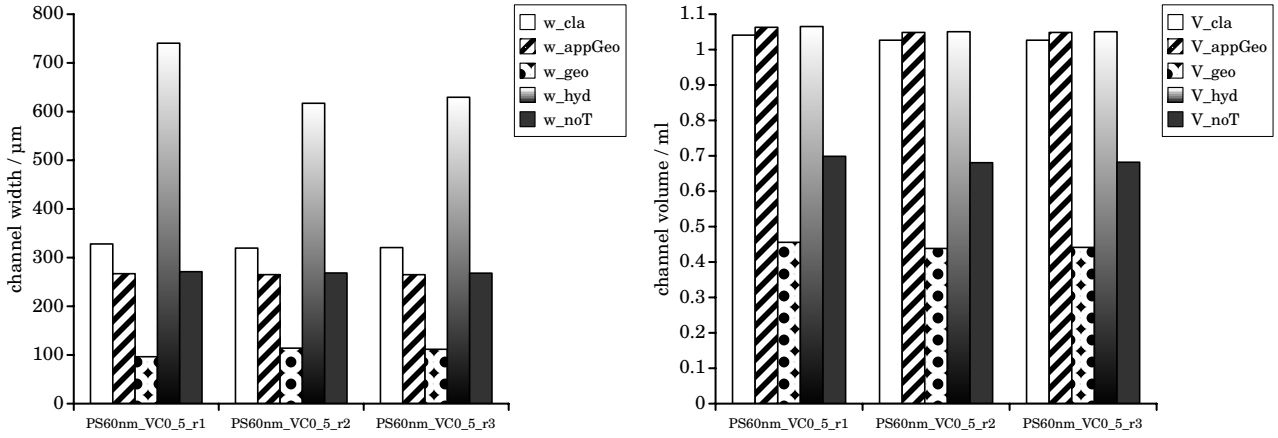

(a) Calibration results for w (b) Calibration results for V

Fig. S.6.17: Results of w and V from all 5 calibration algorithms for PS measurements at $\dot{V}_c = 0.5\,^{\mathrm{ml}}/_{\mathrm{min}}$, $z_{\%} = 16\,\%$

Single results of calibration experiments with literature data, $z_{\%} = 8\,\%$

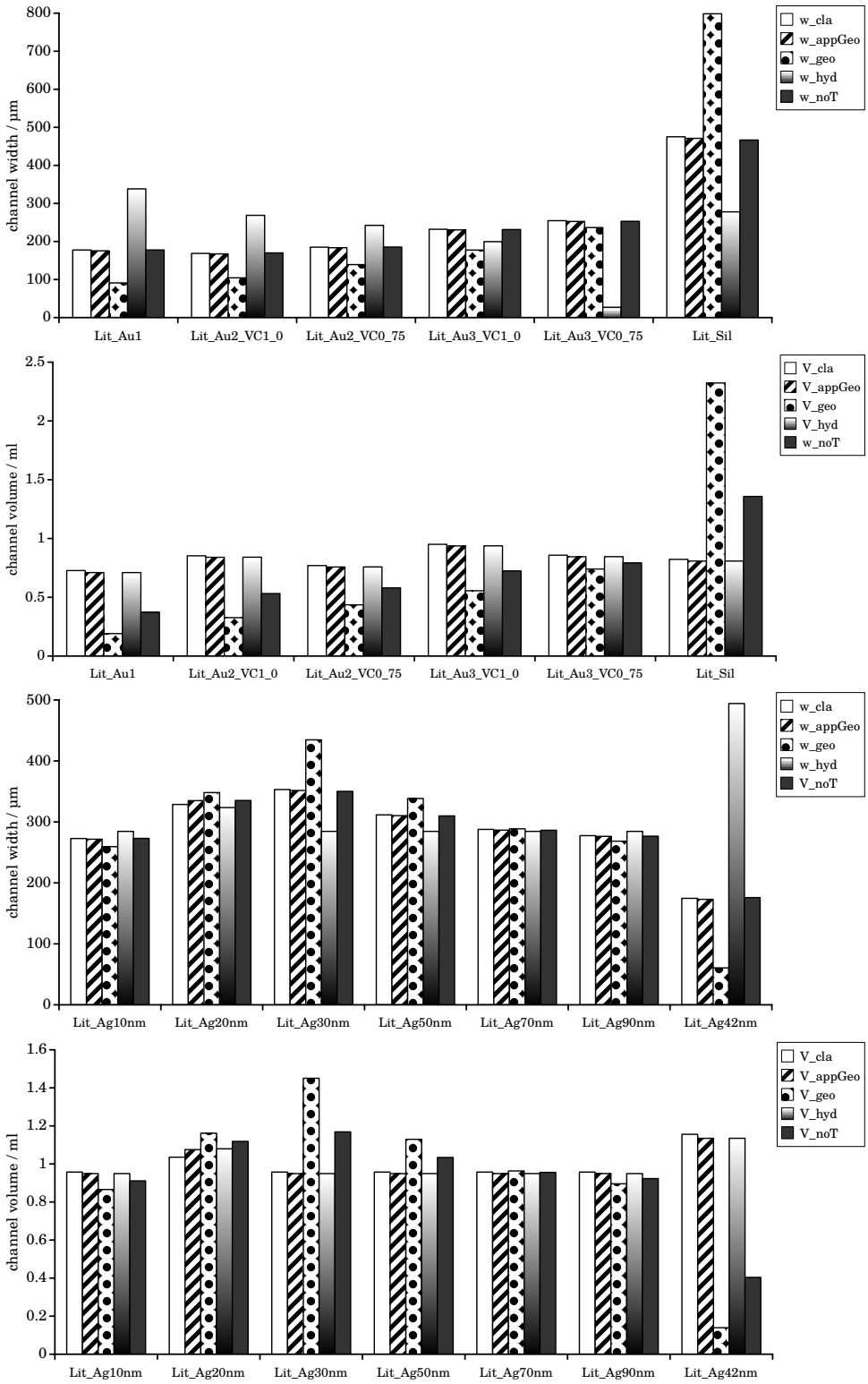

a: w for data from Table

Fig. S.6.18: Results of calibration algorithms with literature data

Single results of calibration experiments with literature data, $z_{\%} = 16\,\%$

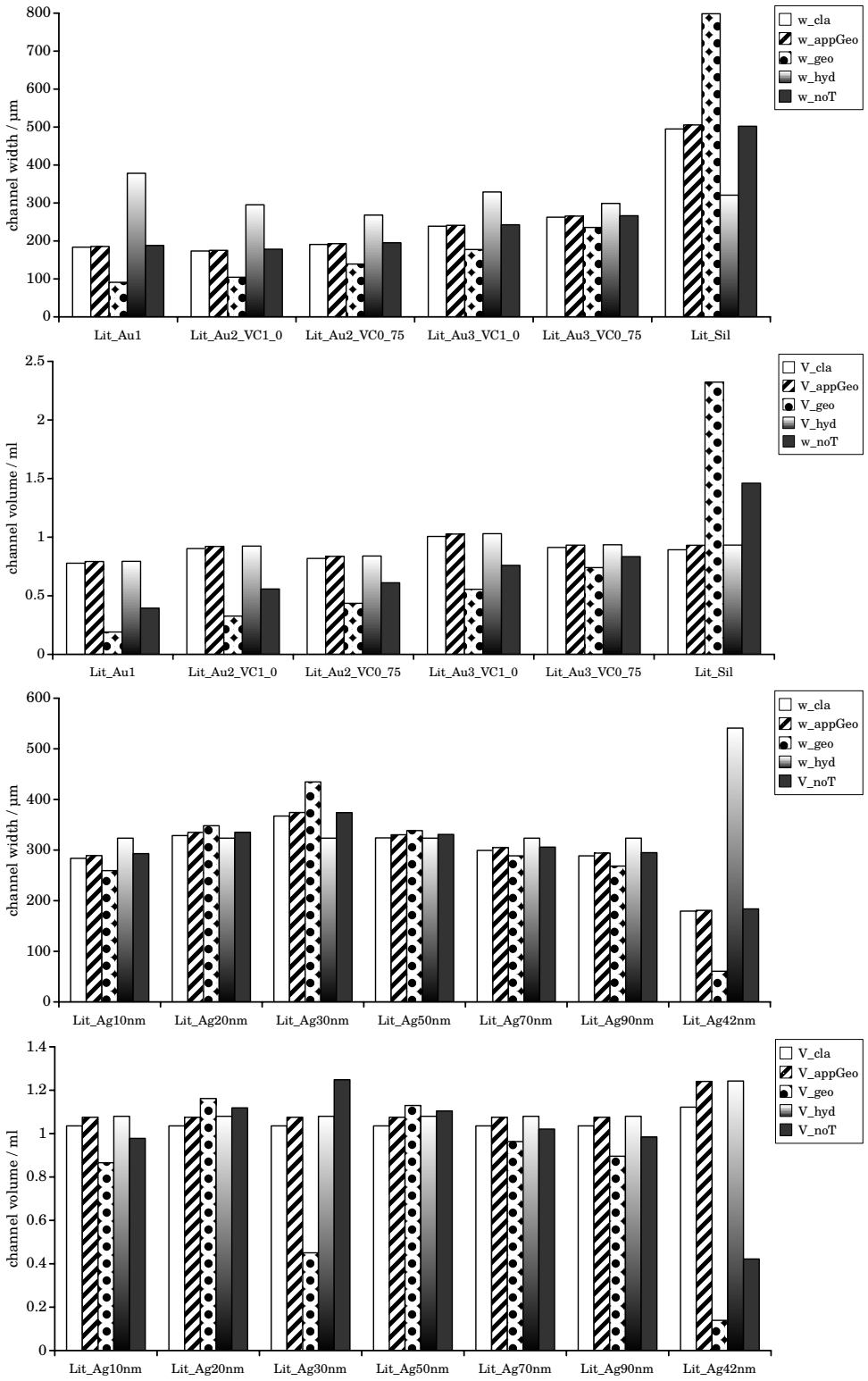

a: w for data from Table

Fig. S.6.19: Results of calibration algorithms with literature data

Deviation influences

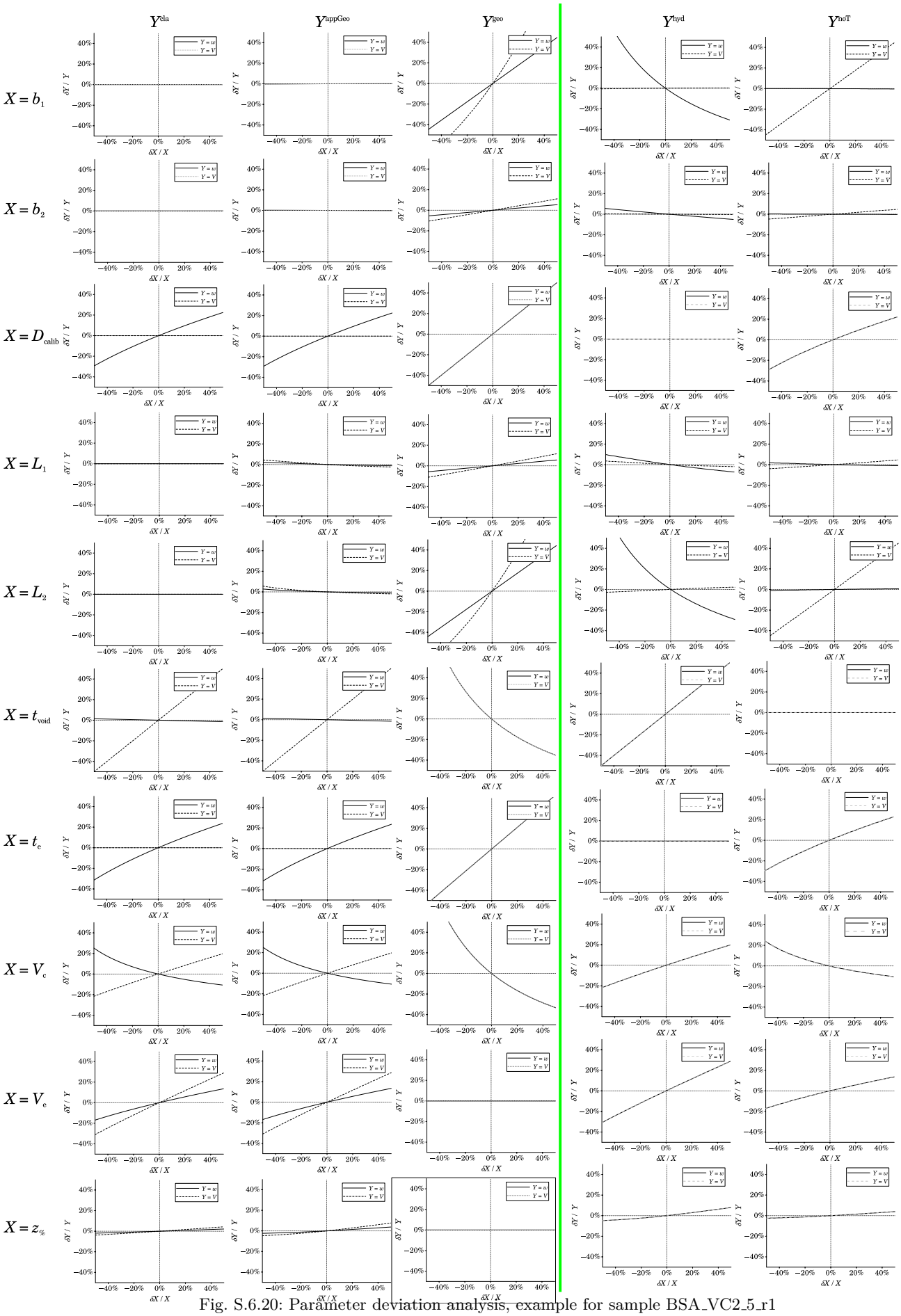

Fig. S.6.20: Parameter deviation analysis, example for sample BSA_VC2_5_r1

Single results of own calibration experiments with calculated t_{void}, $z_{\%} = 12\,\%$

(a) Calibration results for w (b) Calibration results for V

Fig. S.6.21: Results of w and V from all 5 calibration algorithms for BSA measurements at $\dot{V}_{\text{c}} = 2.5\,{}^{\text{ml}}/_{\text{min}}$, $z_{\%} = 16\,\%$

(a) Calibration results for w (b) Calibration results for V

Fig. S.6.22: Results of w and V from all 5 calibration algorithms for BSA measurements at $\dot{V}_{\text{c}} = 3.5\,{}^{\text{ml}}/_{\text{min}}$, $z_{\%} = 16\,\%$

(a) Calibration results for w (b) Calibration results for V

Fig. S.6.23: Results of w and V from all 5 calibration algorithms for PS measurements at $\dot{V}_{\text{c}} = 0.5\,{}^{\text{ml}}/_{\text{min}}$, $z_{\%} = 16\,\%$

7 Detailed measurement program

Table S.7.1: Steps of the measurements series BSA_VC2_5, $\dot{V}_e = 1\,^{ml}/_{min}$

Step	start time	mode	crossflow	focus flow
	min	E = Elution, F = Focus, I = Injection	in $^{ml}/_{min}$	
	0	E	-	-
	1	E	2.5	-
Focussing	3	F	-	1.5
	4	F&I	-	1.5
Separation	8	E	2.5	-
	43	E&I	-	-
	48	E	-	-

Table S.7.2: Steps of the measurements series BSA_VC3_5, $\dot{V}_e = 1\,^{ml}/_{min}$

Step	start time	mode	crossflow	focus flow
	min	E = Elution, F = Focus, I = Injection	in $^{ml}/_{min}$	
	0	E	-	-
	1	E	3.5	-
Focussing	3	F	-	1.5
	4	F&I	-	1.5
Separation	8	E	3.5	-
	43	E&I	-	-
	48	E	-	-

Table S.7.3: Steps of the measurements series PS_VC0_5, $\dot{V}_e = 1\,^{ml}/_{min}$

Step	start time	mode	crossflow	focus flow
	min	E = Elution, F = Focus, I = Injection	in $^{ml}/_{min}$	
	0	E	-	-
	1	E	0.5	-
Focussing	3	F	-	1.5
	4	F&I	-	1.5
Separation	8	E	0.5	-
	43	E&I	-	-
	48	E	-	-

References

[1] K.-G. Wahlund, *Journal of chromatography. A* **2013**, *1287*, 97–112.

[2] E. Magnusson, A. Håkansson, J. Janiak, B. Bergenståhl, L. Nilsson, *Journal of chromatography. A* **2012**, *1253*, 127–133.

[3] H. Bolinsson, Y. Lu, S. Hall, L. Nilsson, A. Hakansson, *Journal of chromatography. A* **2018**, *1533*, 155–163.

[4] A. Håkansson, E. Magnusson, B. Bergenståhl, L. Nilsson, *Journal of chromatography. A* **2012**, *1253*, 120–126.

[5] K. G. Wahlund, J. C. Giddings, *Anal Chem* **1987**, *59*, 1332–1339.

[6] A. Litzén, K.-G. Wahlund, *Anal. Chem.* **1991**, *63*, (Ed.: P. A. Jansson), 1001–1007.

[7] I. Bronstein, K. Semendjajew, G. Musiol, H. Mühlig in *Taschenbuch der Mathematik*, Harri Deutsch, **2008**, Chapter 21.7.1.2, p. 1077.

[8] I. Bronstein, K. Semendjajew, G. Musiol, H. Mühlig in *Taschenbuch der Mathematik*, Harri Deutsch, **2008**, Chapter 21.7.1.2, p. 1076.